AD-A127 492 FRACTURE BEHAVIOR OF BORON ALUMINUM COMPOSITES AT ROOM AND ELEVATED TEMPE..(U) DREXEL UNIV PHILADELPHIA PA DEPT OF MECHANICAL ENGINEERING AN.. J AWERBUCH OCT 82 1/1

UNCLASSIFIED AFOSR-TR-83-0269 AFOSR-79-0079 F/G 11/4 NL

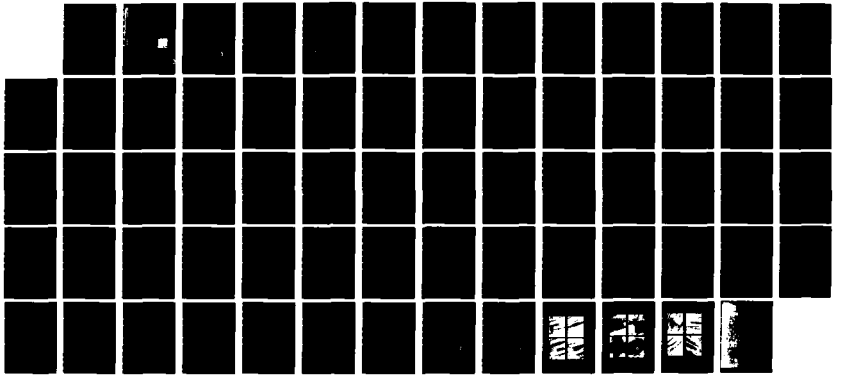

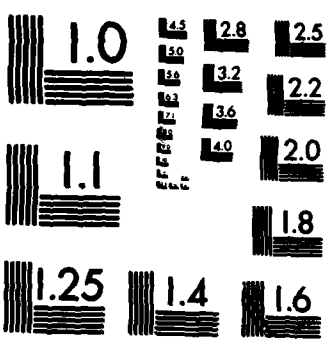

FRACTURE BEHAVIOR OF BORON ALUMINUM COMPOSITES AT ROOM AND ELEVATED TEMPERATURES

Drexel University

College of Engineering
Department of
Mechanical Engineering
and Mechanics
Philadelphia, PA 19104

(215)895-2352-53

FRACTURE BEHAVIOR OF BORON ALUMINUM COMPOSITES AT ROOM AND ELEVATED TEMPERATURES

PROGRESS REPORT

Grant AFOSR -79-0079

PERIOD: JUNE 1, 1980 - MAY 31, 1981

Submitted by

Dr. Jonathan Awerbuch

Department of Mechanical Engineering and Mechanics
Drexel University
Philadelphia, Pennsylvania
19104

UNCLASSIFIED

SECURITY CLASSIFICATION OF THIS PAGE (When Data Entered)

REPORT DOCUMENTATION PAGE		READ INSTRUCTIONS BEFORE COMPLETING FORM
1. REPORT NUMBER **AFOSR-TR- 83-0269**	2. GOVT ACCESSION NO.	3. RECIPIENT'S CATALOG NUMBER
4. TITLE (and Subtitle) FRACTURE BEHAVIOR OF BORON ALUMINUM COMPOSITES AT ROOM AND ELEVATED TEMPERATURES		5. TYPE OF REPORT & PERIOD COVERED Annual 1 Jun 80 - 31 May 81
		6. PERFORMING ORG. REPORT NUMBER
7. AUTHOR(s) JONATHAN AWERBUCH		8. CONTRACT OR GRANT NUMBER(s) AFOSR-79-0079
9. PERFORMING ORGANIZATION NAME AND ADDRESS DREXEL UNIVERSITY DEPARTMENT OF MECHANICAL ENGINEERING & MECHANICS PHILADELPHIA, PA 19104		10. PROGRAM ELEMENT, PROJECT, TASK AREA & WORK UNIT NUMBERS 61102F 2307/B2
11. CONTROLLING OFFICE NAME AND ADDRESS AIR FORCE OFFICE OF SCIENTIFIC RESEARCH/NA BOLLING AFB, DC 20332		12. REPORT DATE October 1982
		13. NUMBER OF PAGES 63
14. MONITORING AGENCY NAME & ADDRESS(if different from Controlling Office)		15. SECURITY CLASS. (of this report) UNCLASSIFIED
		15a. DECLASSIFICATION/DOWNGRADING SCHEDULE

16. DISTRIBUTION STATEMENT (of this Report)

Approved for public release; distribution unlimited.

17. DISTRIBUTION STATEMENT (of the abstract entered in Block 20, if different from Report)

18. SUPPLEMENTARY NOTES

19. KEY WORDS (Continue on reverse side if necessary and identify by block number)

FRACTURE	ACOUSTIC EMISSION	FAILURE
BORON/ALUMINUM	COMPOSITE MATERIALS	FRACTOGRAPHY
FAILURE MODES	CRACK PROPAGATION	
NOTCH SENSITIVITY	NOTCHED STRENGTH	
FRACTURE STRENGTH	MECHANICAL PROPERTIES	

20. ABSTRACT (Continue on reverse side if necessary and identify by block number)

This progress report describes the results of research work on the characterization of fracture behavior in boron/aluminum (B/Al) composites. Emphasis has been placed on the correlation between the observed failure modes and the deformation characteristics of center-notched B/Al composites, where particular attention has been given to the proper test procedure and analytical approach employed. The purpose of this work is not merely to generate and furnish quantitative data but also to discuss the appropriate methodology to be employed in characterizing a new composite material system.

DD FORM 1 JAN 73 1473 EDITION OF 1 NOV 65 IS OBSOLETE

UNCLASSIFIED

SECURITY CLASSIFICATION OF THIS PAGE (When Data Entered)

The investigation focused on the deformation characteristics, crack tip damage growth, fracture strength, notch sensitivity, and the associated characterization methods. In the current year program, emphasis has been placed on interfacing the experimental instrumentation with a data acquisition system. A complete description of all experimental procedures and techniques has been given in the previous progress reports. Some of the experimental results are as follows. Load-crack opening displacement (COD) of notched unidirectional boron/aluminum composites behavior becomes increasingly nonlinear above 200°F, attributed primarily to the greater ductility of the aluminum matrix at elevated temperature. There appears to be no temperature effect on elevated temperature notched strength (up to 600°F) of unidirectional (0°) systems governed by fiber strength, whereas for (90°) specimens which are dominated by matrix properties there is an extremely significant effect of elevated temperature. Individual boron fiber fracture strength tests yielded low strength and wide scatter which are the major reasons for the low strength values obtained for the composite. Extensive acoustic emission information is reported and an attempt is made to distinguish among major failure mechanisms, and to monitor fatigue damage progression. Considerable care must be taken to distinguish between emission due to new damage growth and emission due to friction.

TABLE OF CONTENTS

I. SUMMARY

This progress report describes the results of research work on the characterization of fracture behavior in boron/aluminum (B/Al) composites at room and elevated temperatures during the period June 1, 1980 to May 31, 1981. The study has been directed toward the deformation characteristics and notch sensitivity of center-notched B/Al composites and particular attention is given to the proper test procedures and analytical approaches employed.

The overall research program covers many aspects associated with the deformation characteristics and failure mechanisms in a wide variety of center-notched boron/aluminum laminates and unidirectional systems of various constituents. Employing a range of experimental techniques and procedures for comparison purposes, the program has focused on examination of crack tip damage growth, fracture strength and notch sensitivity, failure modes and their associated characterization methods, the effect(s) of constituents on fracture behavior, and microstructural studies. The primary experimental technique has been to utilize the interferometric displacement gage (IDG) through which the actual crack opening displacement (COD) can be measured at room and elevated temperatures, resulting in exact load-COD and local compliance curves. Special attention has also been given to acoustic emission for evaluating internal damage and damage growth. As can be seen from the scope of the research work, the purpose has not been merely to generate quantitative data but also to assess the appropriate methodologies for characterizing a new composite material system.

In the current year program, emphasis has been placed on interfacing the experimental instrumentation with a data acquisition system. Software was developed for real time data acquisition and subsequent data analysis.

Specifically, the interferometric displacement gage was interfaced with the MINC-11 minicomputer allowing for final analysis of local compliance and plotting of load-COD curves, and standard compliance gages and strain gages as well as the acoustic emission instrumentation have also been interfaced with the data acquisition system, the last of which allows monitoring of damage progression during fatigue loading.

This report presents representative data on the fracture behavior of unidirectional boron/aluminum at room and elevated temperatures, preliminary data on the notched strength of B/Al laminates, strength and acoustic emission data of boron filaments, and acoustic emission data on B/Al laminates during quasi-static and low cycle fatigue loading. A complete description of all experimental procedures and techniques has been given in the previous progress reports.

II. INTRODUCTION*

The mechanical behavior of boron/aluminum (B/Al) composites has been studied extensively over the past decade due to an increasing recognition of its advantages in terms of broader operational temperature ranges, higher impact resistance, strength and stiffness, and significantly better transverse and shear properties. Currently, boron/aluminum composites maintain their position as the primary metal matrix composite material for aircraft and aerospace applications based upon superior properties and performance experience [1].

A subject of extreme concern is the fracture behavior of B/Al composites which exhibit extremely low elongation up to fracture, and several studies have addressed this issue [2-8]. The applicability of linear elastic fracture mechanics (LEFM) to unidirectional B/Al has been discussed [2,3,4] with varying conclusions. For example, Kreider and Dardi [2], and Mar [3] concluded that the correlation between fracture strength σ_f and half crack length a is best described by an equation of the form $\sigma_f a^m$ = const. However, contrary to LEFM predictions, the exponent m was found to be less than one half. Wright [4] concluded that LEFM can be applied, provided that the crack extension prior to failure is added to the initial crack length. With this assumption, the data of [4] as well as [2] agree with predictions based on LEFM. This assumption follows, in fact, the analytical models proposed in [5,6] for notched strength predictions of composites. Hancock and Swanson [7] concluded that the conventional concepts of fracture toughness can be useful in characterizing the toughness of unidirectional B/Al. Sun and Prewo [8] showed that the fracture toughness of B/Al can be described by LEFM provided the crack extension is

---

* This introduction first appeared in the former Proposal and is included here for the sake of completeness.

colinear with the initial pre-machined notch, as is the case for [90°] or [0°/90°] laminates of compact tension specimen geometry. For unidirectional B/Al, such an approach is not relevant [8] due to the large amount of plastic deformation of the matrix parallel to the filaments. Similar damage growth and modes of failure under static and fatigue loadings have been observed and discussed in [2,9,10,11]. In general, it has been shown that the failure of unidirectional B/Al is preceded by longitudinal plastic deformation at the crack tip which eventually leads to matrix cracking and crack tip blunting, all of which contribute to the crack arresting mechanism. The incipient matrix cracking has been described by the elastic stress intensity factor [9]. Obviously when different analytical approaches and experimental techniques are employed to define fracture toughness, the resulting toughness values vary significantly. Nevertheless, the majority of the values are still very promising in comparison with other metal or resin matrix composites.

With regard to mechanical properties, attention has been directed primarily toward unidirectional 5.6 mil B/Al-6061F. However, with the more demanding requirements for toughness, recent attention has been given to other material systems, e.g., unidirectional 8.0 mil B/Al-1100F, primarily for jet engine fan blade applications. For such applications, better impact resistant and less notch sensitive material systems are being sought. Charpy test results [12-14] have shown that 8.0 mil B/Al-6061F does demonstrate certain advantages over the more common 5.6 mil B/Al-6061F. The choice of low shear strength matrices such as 1100 aluminum, combined with high strength fibers provides a material system capable of dissipating high levels of energy upon impact loading [12]. Limited studies have also been directed toward the use of B/Al laminates [12,14].

Despite the many studies on the fracture behavior of unidirectional 5.6 mil B/Al-6061F composite, a complete and definitive correlation between the

observed failure modes and the deformation characteristics is lacking. 8.0 mil B/Al-1100F or B/Al laminates have received even less attention with regard to their deformation characteristics and notch sensitivity. Under operational conditions the fracture behavior of all boron/aluminum composite systems remains incomplete and/or unreliable.

The primary objective of this study has been to characterize the fracture behavior of boron/aluminum composites at room and elevated temperatures experimentally and analytically. Examinations include the deformation characteristics of center-notched specimens, change in compliance with crack length at various temperatures, load-displacement curves at various temperatures, fracture strength and notch sensitivity, failure modes, microstructural studies of interfaces, and monitoring of crack tip damage growth. Data to be obtained and procedures to be employed entail:

- Load-crack opening displacement (COD) curves using the laser interferometric displacement gage technique.
- Far-field load-displacement curves using the standard compliance gages.
- Local and global compliance curves.
- K-calibration curves.
- Fracture strength and notch sensitivity.
- Crack tip damage growth, deformation characteristics and failure modes.
- Microstructural analysis of failure modes, e.g., examination of fiber, matrix, and interface by optical and electron microscopy techniques.

- Detection of damage mechanisms and internal damage through X-ray radiography, ultrasonic C-scan, and acoustic emission.
- Monitoring damage growth through acoustic emission, e.g., location and amplitude distribution histograms of events, counts and count rate, and cumulative event amplitude distribution.
- Acoustic emission studies on constituents and "simple" structures.
- Correlating acoustic emission information with actual deformation characteristics and failure modes.
- Fracture behavior of unidirectional versus laminated boron/aluminum.
- Effect(s) of elevated temperatures on fracture behavior.
- Mechanical properties (elastic constants) at room and elevated temperatures.
- Axial splitting in notched unidirectional boron/aluminum.
- Effect(s) of constituents (e.g., fiber, matrix) on fracture behavior.
- Applicability of the resistance curve method (based on COD and displacement measurements) to the various boron/aluminum systems.
- Determining the proper test methodology to be employed in characterizing a new composite material system.
- Comparison of experiments with the associated analyses.

III. PROGRESS DURING THE CURRENT PROGRAM

A brief summary of the work carried out during the current period is given below.

Generally, our research activity expanded along the directions outlined on pages 5 and 6 of this Report covering a variety of issues which are all directly related to the understanding of the fracture behavior of boron/aluminum composites. Subjects which received emphasis were compliance curves and load-crack opening displacement curves, crack tip damage growth and failure modes, fracture strength and notch sensitivity, monitoring damage growth during quasi-static loading and damage accumulation during fatigue loading by means of acoustic emission, and microstructural studies using scanning electron microscopy and photomicrography. All these studies (besides the acoustic emission monitoring) were conducted at room and elevated temperatures, primarily on unidirectional boron/aluminum, with some preliminary studies on boron/aluminum laminates.

The progress to date and some representative results are given in this section.

A. Preparation of Laboratory Facilities

The experimental procedures employed in this program include a variety of techniques from which the material mechanical properties, fracture behavior, deformation characteristics, damage accumulation and failure modes were examined. These techniques include: laser interferometric displacement gage, strain gages, extensometers, acoustic emission, X-ray radiography, scanning electron microscopy, data acquisition systems, etc. These techniques were developed during the initial phase of this program during which period specific facilities were purchased, as described in Section II of the previous Progress

Report.

During this period emphasis has been placed on expediting the data reduction and analyses schemes. For this purpose significant time and effort has been spent to interface the data acquisition system (PDP 1103 Model MINC-11) with several of the laboratory components, for example:

1. The laser interferometric displacement gage (IDG): with the IDG, the actual crack opening displacement (COD) can be measured very accurately on the sub-micron scale. The COD is obtained as a function of time, and when correlated with the load-time curve obtained from the Instron's load-cell, highly detailed load-COD curves can be reduced. The manual data reduction scheme is very time consuming, therefore a successful attempt has been made to interface the IDG with the data acquisition system. Now the whole process of data acquisition, reduction, analysis and plotting (Hi-plot plotter) is automated, resulting in final results of local compliances and load-COD curves. A detailed computer program prepared by our laboratories is provided as an Appendix to this Report and is submitted separately. Certain modifications of the program, such as monitoring crack tip damage growth through compliance matching, are underway.

2. Compliance Gage and Strain Gages: the monitoring of displacements by means of compliance gages and strain gages have also been interfaced with the data acquisition system. Again, load-displacement curves, global compliances, stress-strain curves and mechanical properties (such as strength and stiffness) are monitored during the test and data are recorded, reduced, analyzed and plotted by the MINC-11. A detailed computer program for this scheme is also provided in the separate Appendix.

3. Acoustic Emission During Fatigue Loading: the Dunegan/Endevco 3000 series system has been interfaced with the data acquisition system for the purpose of monitoring damage progression during fatigue loading.

A separate computer program has been developed through which the number of events and number of events per load cycle at different load levels are recorded. The recorded data are reduced, analyzed and plotted, resulting in plots of events and events per cycle as a function of number of cycles at different load levels. The details of this computer program are also provided in the separate Appendix.

B. Materials

All material to be tested in this program has been purchased and machined. Two types of specimens are tested: center-notched specimens 200 x 25 mm (8.0 x 1.0 inch), and unnotched specimens 200 x 13 mm (8.0 x 0.5 inch). The total number of specimens for each material system has been outlined in the former Proposal and Progress Report. The specimen preparation procedures include measurements, tabbing and the introduction of micro-indentations to those specimens to be tested with the IDG.

C. Mechanical Properties

The elastic stiffnesses and strength for unidirectional systems were obtained experimentally at room and elevated temperatures, as outlined in Tables I and II. In addition, basic fiber properties (5.6 mil and 8.0 mil diameters) were tested for strength, Table III. The scatter in strength has been characterized for the composite and individual fiber data of Tables I and III using the two-parameter Weibull distribution, Figures 1 and 2. Acoustic emission distributions of events for the individual fibers (5.6 mil and 8.0 mil diameters) were correlated with those obtained for various boron/aluminum composite systems, and a detailed discussion of the acoustic emission testing and results is given in part I of this section. A selected number of tests were also performed on aluminum matrices manufactured through a process identical to that used for the composite material.

D. Elevated Temperature Compliance Curves

Local compliance curves obtained with the IDG at room and elevated temperatures were obtained for various notch lengths. As mentioned in part A, the IDG has been interfaced with a data acquisition system. Typical outputs are shown in Figures 3 and 4 for notched unidirectional 5.6 mil 6061F boron/aluminum at 21°C (70°F) and 316°C (600°F), respectively. The standard procedure of the test program is for each specimen to be loaded to approximately 5% of the expected ultimate load, and then unloaded. This loading/unloading cycle is repeated three to six times. The local compliance is calculated for each of the load cycles, the average of which is used in the subsequent analyses. As shown in Figures 3 and 4, the results are highly reproducible with very small standard deviation, Table IV. This technique is easily applied in elevated temperature measurements as well, Figure 4. Similar results were obtained for $[90°]_8$ specimens, Figures 5 and 6 for 21°C and 316°C, respectively, although the displacement is much smaller due to the low load levels that can be applied within the elastic region. Results are also very reproducible for these cases, Figures 5 and 6 and Table IV. A summary of the results for $[0°]_8$ specimens is shown in Figure 7 and Table V at different temperatures. It should be noted that the large scatter in data prevented a distinction of the effect of temperature on compliance. Therefore, the local compliance measurements were carried out on the same specimens at different temperatures, Figure 8. A significant effect of temperature on local compliance is clearly observed, beginning at temperatures of 260°C (500°F), Table IV and Figures 9 and 10. In order to be able to predict this dependency on temperature, the variation of transverse and shear moduli with temperature must be established for the subject material, and this testing is planned for execution in the next phase of the program. Data on the global compliance tests obtained with the compliance gage are given in Table VI.

E. Elevated Temperature Load-COD Curves

The effect of elevated temperatures on the deformation characteristics of notched $[0°]_8$ and $[90°]_8$ has been investigated. Load-COD curves at different temperatures are shown in Figure 11 for unidirectional 5.6 mil B/Al 6061F. A significant effect of temperature on the deformation characteristics and notch tip damage growth appears at temperatures above 93°C (200°F). At the higher temperatures there is an increase in non-linearity in the load-COD curve, resulting in large COD at failure. Both the nonlinearity in the load-COD curve and the large COD at failure are attributed primarily to the greater ductility of the aluminum matrix at these elevated temperatures. Note that the typical failure mode at the crack tip is matrix shear plastic deformation along the fibers and in the loading direction. In other words, differences between the curves indicates much larger crack tip damage growth at elevated temperatures which results from the elevated temperature properties of the matrix material. A variation in fiber-matrix interface properties at higher temperatures might also have some effect.

For predicting the load-COD curve at elevated temperatures, a model suggested by [22] and successfully applied for room-temperature load-COD curves in [18] has been used. In applying this model, an appropriate yield shear stress of the aluminum matrix, τ_m, must be selected. The experimental load-COD curves were compared with theory, using different values of τ_m at the given test temperatures and it seems that a good correlation can be established, Figure 11. It should be noted that the values of τ_m given in the table of Figure 11 were chosen arbitrarily to fit the data. Additional testing is warranted to determine the actual yield shear strength of aluminum at different temperatures. However, a good agreement has been established for various notch lengths with similar values of τ_m.

F. Fracture Strength and Notch Sensitivity at Elevated Temperatures

Notched strength of unidirectional $[0°]_8$ and $[90°]_8$ 5.6 mil B/Al 606IF at elevated temperatures up to 314°C (600°F) have been recorded, Tables VII and VIII. The results for the unidirectional specimens indicate that up to the maximum applied temperature neither axial strength nor axial stiffness degradation is observed, Tables I, VII and Figure 13. The elevated temperature notch strength data fall well within the scatter of the room temperature data, Figure 13. In other words, there appears to be no effect of temperature on the fiber controlled properties. On the other hand, the experimental results for the transverse $[90°]_8$ specimens demonstrate significant dependence of notched strength on temperature, Table VIII, indicating again the effect of matrix controlled properties on the fracture behavior of the subject material.

G. Notch Sensitivity of Boron/Aluminum Laminates

Preliminary tests on the notched strength of a variety of boron/aluminum laminates have been conducted in which global compliances, fracture strength and acoustic emission data have been recorded. Notched strength data for the $[0/50]_{2s}$ laminate indicate significant notch sensitivity. A comparison of the notched strength and global compliances for the various laminates ($2a/W = 0.2$) shows the significant influence of laminate configuration. The data shown in Table IX indicates the importance of pursuing broader studies into the fracture behavior of boron/aluminum laminates both at room and elevated temperatures. Such studies will constitute a major effort during the next phase of this research program.

H. Constituent Properties

In order to evaluate the global mechanical properties and fracture behavior of the subject boron/aluminum composites, emphasis has also been placed on the constituent properties. For this purpose, representative fibers

used in the fabrication of each plate were purchased along with aluminum plates that were fabricated by the same procedure as the boron/aluminum composite plates.

A total of 19 fibers 5.6 mil in diameter and 17 fibers 8.0 mil in diameter were tested for ultimate strength and acoustic emission amplitude levels, Table III. Note the very large scatter and low average of the fiber strength. The data from Table I for composite strength and the data from Table III for the fiber strength were fitted to the two-parameter Weibull distribution function, Figures 1 and 2, indicating very low shape and scale parameters. A comparison of Figures 1 and 2 explains the relatively low strength of the unidirectional 5.6 mil boron/aluminum 6061F tested in this program. The same conclusion can also be shown by applying the elementary rule of mixtures using the 45% volume fraction of the fibers in the composite plates.

I. Acoustic Emission

Additional testing was performed on monitoring acoustic emission in boron/aluminum. These studies focused on the potential of using acoustic emission to identify failure modes in different boron/aluminum laminates and to monitor damage progression during low cycle fatigue loading.

The identification of the major failure mechanisms, namely fiber failure and matrix plastic deformation, was attempted by analyzing the amplitude distribution histograms of events for individual fibers and for a variety of boron/aluminum laminates. The results for the individual fibers indicate that practically all fiber fractures are associated with very high amplitude levels of events, i.e., 95 to 98 dB, as indicated in Table III. Figures 14 to 19 show the amplitude distribution histograms of events for notched $[0°]_8$, $[90°]_8$, $[0/90]_{2s}$, $[\pm 45]_{2s}$, $[0_2/\pm 45]_s$ and $[0/+45/-45/90]_s$ 5.6 mil boron/aluminum

6061 laminates, respectively. Clearly, each of the laminates results in a different amplitude distribution histogram.

Acoustic emission was also monitored during fatigue loading. Fatigue tests are performed under load control mode at a frequency of 1.0 Hz up to a maximum of 5000 cycles. The fatigue stress ratio was set at 0.1. Examination of the acoustic emission data (as well as observations of crack tip damage growth via the closed-circuit television system described in part J) indicate that initially most of the emission occurs at the maximum load level. However, as the number of cycles progresses, a large percentage of the emission occurs during unloading and during loading at load levels much below the maximum load level. This indicates that not all of the emission accumulated during the fatigue loading is necessarily emitted from newly created damage surfaces, but is due rather to friction between existing fracture surfaces and is caused by crack closure during the fatigue loading.

Generally, it was determined during the initial phase of the program that a significant amount of emission was due to such existing damage. Therefore special efforts were made to distinguish the emission caused by newly created damage from that caused by friction among existing fracture surfaces. A computer program was developed for the MINC-11 data acquisition system to monitor acoustic emission during fatigue loading. The program also monitors the number of events accumulated at a predetermined load range for each load cycle. The details of this computer program are given in the Appendix to this report.

The predetermined load ranges were set arbitrarily at 60%, 80% and 95% of the maximum fatigue load (P_{max}), and events accumulated throughout the load cycle (0-100% of P_{max}) and those accumulated in the 60-100%, 80-100% and 95-100% of P_{max} were plotted as shown in Figure 20. To emphasize the amount of

emission occurring at low load level ranges (and attributed to friction) the events accumulated during 0-60%, 0-80% and 0-95% are shown as well. The amount of emission occurring due to friction is therefore clearly seen in Figure 20. The table shown in Figure 20 displays the dynamic stress level, σ_D, the number of events occurring in the first cycle, E_o, and those occurring during the fatigue loading, E_n. In order to amplify the variation in emission during the fatigue loading, the slopes of the curves shown in Figure 20 were calculated and plotted in Figures 21 and 22. The amount of emission occurring at low load levels, i.e., emission due primarily to friction, is clearly indicated. Figures 21 and 22 also indicate the pattern of damage progression. It is clearly seen from Figure 21 that sudden damage increases occur at approximately 500, 900, 1400, 1900 and 2400 cycles, which can be correlated with the actual progression of splitting. The correlation is verified through both the location distribution histogram of events and the visual observation of damage progression via the closed-circuit television system.

Generally, from the plots such as those shown in Figures 20 to 22, the cycle number at which a sudden damage growth takes place can be readily and precisely determined. From the location distribution histogram of events (not shown here) the approximate location at which the damage occurs can be determined as well. The amplitude distribution histograms such as those shown in Figures 14 to 19 might provide clues as to the type of damage occurring. In other words, it seems that the monitoring of damage progression during fatigue loading by means of acoustic emission provides a simple test procedure by which we can determine "when" and "where" damage occurs and it holds potential for determining "why" damage occurred, though only on the qualitative level at this stage. By applying acoustic emission to the test specimen, decisions concerning when and where to conduct more detailed NDT examinations such as ultrasonic C-scan, X-ray radiography, replica technique, etc., can be

readily made and consequently result in a savings of time and money.

J. Visual Monitoring of Damage Progression

Recently, a closed-circuit television system (CCTV) was purchased, with a microscope attached to the camera which allows magnification up to 250 X. Damage progression during static and fatigue loading can be directly observed via the CCTV, the type of predominant damage is identifiable and location and damage progression can be precisely detected and tracked. A qualitative correlation between the damage progression observed through the CCTV and the acoustic emission information (as described in part I) was easily established.

K. Failure Modes and Fracture Surfaces

Fracture surfaces of notched and unnotched unidirectional and transverse specimens, subjected to various elevated temperatures, were examined through the scanning electron microscope (SEM). The purpose of these examinations was three-fold: 1) to evaluate the fabrication quality of the specimen material tested; 2) to study the effect of elevated temperatures on the fracture surface morphology; and 3) to examine the dominant micro-failure mechanisms.

Generally, the SEM studies indicate very good fiber-matrix and matrix-matrix bonding. The low strength of the composites tested cannot be attributed to the fabrication quality or procedures. The predominant factor in the low strength is therefore the poor quality of the fibers used in fabricating the composites plates, as was shown in part G. It seems therefore that quality control testing and examination should always include an evaluation of representative fibers used in the fabrication of any structural element before it is fabricated.

Practically no fiber pull-out in the $[0°]_8$ specimens or fiber splitting in the $[90°]_8$ specimens was observed. The fibers in the $[0°]_8$ are fragmented

into wedge-shaped fragments, however this shattering does not extend over a distance larger than two fiber-diameters.

No significant effect of elevated temperatures (up to 316°C, 600°F) on the fracture surface morphologies has been noticed. For the $[0°]_8$ specimens, SEM examinations reveal no distinction between the micro-failure modes of specimens tested at room temperature and those tested at 316°C (600°F). The SEM examinations were directed toward the amount of fiber pull-out, fracture surfaces of the broken fibers, fiber-matrix and matrix-matrix bonding, plastic deformation and micro-yielding of the aluminum matrix etc. as shown in Figures 23 and 24. For the $[90°]_8$ specimens the major distinction which appeared between the room and elevated temperature morphologies was the amount of micro-void coalescence noticed at room temperature, while at elevated temperatures specimens exhibited a much higher degree of matrix plastic deformation, Figure 25. The effect of temperature on fiber-matrix bonding was inconclusive.

L. Results and Conclusions

We have presented the highlights of our current program on the various aspects of the fracture behavior, deformation characteristics and failure modes of boron/aluminum. It has been demonstrated that the testing methodology employed in this program, namely the use of a variety of experimental techniques, is pertinent and even necessary to the study of a composite material system. A summary of the procedures, results and conclusions is given below:

1. Experimental Set-Up

a. Computer programs for data acquisition, reduction and analyses were successfully developed and employed. These include primarily the following three programs: 1. data acquisition program for the laser interferometric displacement gage (IDG) including data reduction, plotting and analyses to obtain load-COD curves and local compliances at room and elevated temperatures;

2. data acquisition program for compliance gage and strain gages including data reduction, plotting and analyses to obtain far-field load-displacement curves and stress-strain diagrams at room and elevated temperatures; and
3. data acquisition program to monitor damage progression during fatigue loading through acoustic emission, including data reduction and plotting of acoustic emission events and event per load cycle as a function of number of cycles at various load levels during the fatigue loading.

b. A closed-circuit television system was introduced to visually monitor damage progression during fatigue loading. Magnification up to 250 X is available, enabling us to follow the damage progression, damage patterns and damage location.

c. All other test techniques are described in the preceding Progress Report and are successfully and continuously utilized. Particularly the laser interferometric displacement gage technique has demonstrated its usefullness in crack opening displacement measurments at elevated temperatures up to 371°C (700°F).

2. Compliance Curves: local compliance curves at temperatures up to 371°C (700°F) were obtained for various notch lengths.

3. Fracture Strength: results indicate relatively low unnotched strength for unidirectional material. The results of testing on individual boron fibers indicate that their low strength is the major reason for the low strength values obtained for the composite.

4. Notched Strength: elevated temperature notched strength results for unidirectional $[0°]_8$ systems indicate that there is no effect of temperature on notched strength. For $[90°]_8$ specimens, however, a significant effect of

elevated temperatures has been observed.

5. Load-COD Curves: experimental load-COD curves were obtained and successfully compared with analytical model. A significant effect of elevated temperature on load-COD curves was observed.

6. Fracture Surface and Crack Tip Damage:

a. in unidirectional $[0°]_8$ specimens irregular fracture surfaces are observed, resulting from the pattern of the crack tip damage growth. This crack tip damage appears in the form of plastic deformation in the fiber direction. The plastic deformation zones multiply as the load increases. Under fatigue loading, axial splitting is observed (via the CCTV), and a slow crack tip damage growth as the number of cycles progresses.

b. in transverse $[90°]_8$ specimens, self-similar crack tip damage growth is observed, resulting in a fairly coplanar and regular fracture surface.

7. Failure Modes:

a. for unidirectional $[0°]_8$, examination of fracture surfaces reveals a strong fiber-matrix interfacial bond with no fiber-matrix debonding at either room or elevated temperatures.

b. for transverse $[90°]_8$ specimens, a large amount of matrix plastic deformation at elevated temperatures is observed.

8. Acoustic emission information obtained includes accumulative counts and events, count rate and counts per event all as a function of load, displacement and number of cycles, location and amplitude distribution histograms, and cumulative event amplitude distributions, at different load levels and number of cycles.

9. Acoustic emission amplitude distribution histograms obtained for a variety of boron/aluminum laminates indicate the potential for distinguising among the major failure mechanisms, e.g. testing individual boron fibers clearly indicates that fiber fracture results in high amplitude levels while matrix plastic deformation yielded low amplitude acoustic emission events.

10. Emission is obtained during fatigue loading. The amount and rate of emission depends strongly on the dynamic stress level.

11. Monitoring acoustic emission during fatigue loading can indicate damage progression, and it demonstrates potential for forecasting the number of cycles to failure. This technique may also save time and money in studies of fatigue damage initiation and progression in composite systems.

12. Acoustic emission events during fatigue loading do not necessarily mean additional damage; friction among existing fracture surfaces can be a major source of acoustic emission.

13. Acoustic emission tests should be carried out with consistent instrumentation settings, transducers, ultrasonic couplants, tabs, etc. which are to be determined by preliminary testing.

14. The application of acoustic emission technique should be extended to other areas of interest. Areas of importance might be fabrication procedures, impact damage, post-fatigue residual strength, guaranteeing minimum life through monitoring acoustic emission during proof-testing, and reducing scatter in life.

M. Research Activity, Publications and Presentations

1. J. Awerbuch (Principal Investigator)

Dr. Jonathan Awerbuch took a six-month leave of absence (April 1, 1981 to September 30, 1981) to conduct research work at the German Aerospace Research Establishment (DFVLR), in their Institute of Structural Mechanics, Braunschweig, Federal Republic of Germany. During his research work he conducted a detailed and comprehensive investigation into the potential of utilizing acoustic emission technique to monitor damage progression in a variety of graphite/epoxy composite laminates. The results of his work in Germany have been compiled into nine internal reports, one conference proceedings, and several seminars given in research institutes and industries in Germany and the United States, as listed below.

"Investigation of Acoustic Emission in Off-Axis Graphite/Epoxy Composites," DFVLR, ISM (I.B. 131-81/21) 1981.

"Monitoring Damage Progression Through Acoustic Emission in $[\pm 45]_{2s}$ Graphite/Epoxy Laminate", DFVLR, ISM (I.B. 131-81/22), 1981.

"The Effect of Stacking Sequence in Cross-Ply Graphite/Epoxy Laminate on Acoustic Emission Results", DFVLR, ISM (I.B. 131-81/23), 1981.

"Damage Detection in Notched Unidirectional Graphite/Epoxy Through Acoustic Emission," DFVLR, ISM, (I.B. 131-81/24), 1981.

"Monitoring Damage Progression in Notched Unidirectional Graphite/Epoxy During Quasi-Static Cyclic Loading Using Acoustic Emission", DFVLR, ISM (I.B. 131-81/25), 1981.

"Acoustic Emission Monitoring of Damage in Notched $[0_2/+45/0_2/-45/0/90]_{2s}$ Graphite/Epoxy Laminate", DFVLR, ISM (I.B. 131-81/26), 1981.

"Effects of Test Conditions on Monitoring Acoustic Emission in Graphite/Epoxy Laminates", DFVLR, ISM (I.B. 131-81/27), 1981.

"Amplitude Distribution of Acoustic Emission Events in Graphite/Epoxy Laminates", DFVLR, ISM (I.B. 131-81/28), 1981.

"Monitoring Acoustic Emission in Adhesive Bonded Aluminum Lap Joints", DFVLR, ISM (I.B. 131-81/29), 1981.

"Monitoring of Damage Progression in CFRP by Acoustic Emission," presented in the Strukturmechnik-Kolloquium 1981 on "Schadensmechanik von Fasterverstärkten Verbundstrukturen," DFVLR, Institut für Strukturmechanik Braunschweig, Federal Republic of Germany, June 25, 1981.

Ibid, in a seminar given at Messerschmitt-Bölkow-Blohm GMBH, Ottobrunn, Federal Republic of Germany, July 27, 1981.

Ibid, in a seminar given at the Institut für Zerstörungs-freie Prüfverfahren, Fraunhofer-Gesellschaft, Saarbrücken, Federal Republic of Germany (The Institute for Nondestructive Testing), August 31, 1981.

Ibid, in a seminar given at Laboratorium für Betriebsfestigkeit, Fraunhofer Gesellschaft, Darmstadt, Federal Republic of Germany (Laboratory for Fatigue Behavior), September 2, 1981.

"Failure Modes and Acoustic Emission in Composite Materials," a lecture given to the Carl-Cranz Gesellschaft in "Festigkeit und Gestaltung von Bauteilen aus Faserverbundwerkstoffen," Braunschweig, Federal Republic of Germany, September 17, 1981.

"Potential of Acoustic Emission in Monitoring Damage in Composite Materials", seminar given at the Air Force Materials Laboratory, Wright Patterson AFB, Dayton, Ohio, November 5, 1981.

His work on the fracture behavior of boron/aluminum composites have been presented and published as follows:

"Notch Sensitivity of Boron Aluminum Laminate", presented in the 5th Annual Conference on Composites and Advanced Ceramic Materials, The American Ceramic Society, Cocoa Beach, Florida, January 18-22, 1981.

"Fracture Behavior of Unidirectional 5.6/6061 Boron/Aluminum at Room and Elevated Temperatures" in "Mechanics of Composites Review" (Workshop), Dayton, Ohio, October 28, 1981.

2. Dr. M. J. Koczak (Research Associate)

Dr. Koczak's research activity has focused in the area of physical metallurgy, specifically phase and thermodynamic equilibria, diffusion and kinetics as applied to powder metallurgy and metal matrix composite systems. In the area of powder metallurgy, areas of activity include an AFOSR sponsored program on fully dense powder formed Al-Zn-Mg-Co alloys examining the interactions of powder and billet processing, microstructure and mechanical properties,

specifically fatigue response. The program was extended to high temperature Al-Fe-Ni systems under AFOSR support. Three new programs in P/M were initiated (i) an NADC study in high modulus duplex corrosion resistant aluminum P/M alloys, (ii) a second program with NADC in P/M 7000 series alloys and (iii) a study in RSR tool steels under ONR support. In the area of metal matrix composites, Dr. Koczak assists Dr. Jonathan Awerbuch in an AFOSR sponsored B/Al fracture initiation study. In addition, a particulate SiC/Al (7075) study is being initiated at NADC, where student supervision/guidance is provided. Below are listed his publications, presentations, seminars and research activities for this program period.

Aluminum Metal Matrix Composites, AMMRC, Dover, N.J., October 1, 1980.

Metal Matrix Composites - International Harvestor, Chicago, Illinois, February 27, 1980.

Silicon-Carbide-Aluminum Metal Matrix Composites American Ceramic Society Conference, Merritt Island, Florida, January 20, 1981.

Duplex Aluminum Alloys, Drexel University Seminar Series, Philadelphia, PA, November 10, 1981.

Interface Reactions in Metal Matrix Composites, American Ceramic Society Conference, Metal-Ceramics Division, Cocoa Beach, Florida, January 20, 1981.

REFERENCES

1. E. L. Foster, Jr., "Technology Development of Metal Matrix Composites to DOD Application Requirements", proceedings of First MMC Workshop Institute of Defense Analysis, paper P-1144, September 1975.

2. K.G. Kreider and L. Dardi, "Fracture Toughness of Composites", Failure Modes in Composites, I.J. Toth Edt., The Metallurgical Society of the AIME, Vol. I, New York, New York, 1972, pp. 193-220.

3. J.W. Mar and K.Y. Lin, "Fracture Mechanics Correlation for Tensile Failure of Filamentary Composites with Holes", J. of Aircraft, Vol. 14, No. 7, July 1977, pp. 703-704.

4. M.A. Wright and F.A. Iannuzzi, "The Failure of Notched Specimens of Boron-Fiber Reinforced 6061 Aluminum Alloy", Failure Modes in Composites, J.N. Flack and R.L. Mehan, Eds., The Metallurgical Society of the AIME, Vol. II, New York, New York, 1974, pp. 68-94.

5. M.E. Waddoups, J.R. Eisenmann and B.E. Kaminski, "Macroscopic Fracture Mechanics of Advanced Composite Materials", J. Composite Materials, Vol. 5, 1971, pp. 446-454.

6. R.J. Nuismer and J.M. Whitney, "Uniaxial Failure of Composite Laminates Containing Stress Concentrations", in Fracture Mechanics of Composites, ASTM STP 593, American Society of Testing and Materials, 1975, pp. 117-142.

7. J.R. Hancock and G.D. Swanson, "Toughness of Filamentary Boron/Aluminum Composites", Composite Materials: Testing and Design (Second Conference), ASTM STP 497, American Society for Testing and Materials, 1972, pp. 299-310.

8. C.T. Sun and K.M. Prewo, "The Fracture Toughness of Boron Aluminum Composites", J. Composite Materials, Vol. II, 1977, pp. 164-175.

9. W. R. Hoover and R. E. Allred, "The Toughness of Borsic-Aluminum Composites with Weak Fiber Matrix Bonds", Failure Modes in Composites, I.J. Toth Edt., The Metallurgical Society of the AIME, Vol. I, New York, New York, 1972, pp. 311-326.

10. K.M. Prewo and K.G. Kreider, "Fatigue Failure Mechanism in Boron Aluminum", Failure Modes in Composites, I.J. Toth Edt., The Metallurgical Society of the AIME, Vol. I, New York, New York, 1972, pp. 395-413.

11. J.H. Underwood, "Crack-Tip Deformation Measurements Accompanying Fracture in Fibrous and Laminar Composites", Composite Materials Testing and Design (Third Conference), ASTM STP 546, American Society for Testing and Materials, 1974, pp. 376-394.

12. D.L. McDanels and R.A. Signorelli, "Effect of Fiber Diameter and Matrix Alloys on Impact-Resistant Boron/Aluminum Composites", NASA-TN D-8204.

13. K.M. Prewo, "Development of Impact Resistant Metal Matrix Composites", AFML-TR-215, Air Force Materials Laboratory, March, 1976.

14. D.L. McDanels and R.A. Signorelli, "Effect of Angle Flying and Matrix Enhancement on Impact-Resistant Boron/Aluminum Composites", NASA TN D-8205, October 1976.

15. J. Awerbuch, "Deformation Characteristics and Failure Modes of Center Notched Graphite/Epoxy Laminates", to be published.

16. J. Awerbuch, "Fracture Behavior of Boron Aluminum and Borsic Titanium Composites", Progress Report, AFOSR contract #790079, to appear as Air Force Materials Laboratory Technical Report, 1980.

17. J. Awerbuch and H.T. Hahn, "K-Calibration of Unidirectional Metal Matrix Composites", J. Composite Materials, Vol. 12, 1978, pp. 222-237.

18. J. Awerbuch and H.T. Hahn, "Crack-Tip Damage and Toughness of Boron-Aluminum Composites", J. Composite Materials, Vol. 13, 1979, pp. 82-107.

19. J. Awerbuch and H.T. Hahn, "Crack-Tip Damage and Fracture Toughness of Borsic/Titanium Composites", Experimental Mechanics, October 1980, pp. 334-355.

20. J. Awerbuch, "Effect of Constituents on Fracture Behavior of Unidirectional Boron Aluminum Composites", presented in the Symposium on "Fracture Modes in Metal Matrix Composites", the 1980 Annual Meeting of the AIME, Las Vegas, Nevada, February 24-28, 1980.

21. J. Awerbuch, "Notch Sensitivity of Boron Laminate", presented in the 5th Annual Conference on Composites and Advanced Ceramic Materials, The American Ceramic Society, Cocoa Beach, Florida, January 18-22, 1981. To be published.

22. F. A. McClintock, "Problems in Fracture of Composites with Plastic Matrices", presented at the Fourth Symposium on High Performance Composites at St. Louis, MO., Monsanto Co. and Washington University, 1969.

TABLE I: STRENGTH AND STIFFNESSES OF UNNOTCHED BORON ALUMINUM $[0°]_8$ AND $[90°]_8$ 5.6 MIL 6061F AT ROOM AND ELEVATED TEMPERATURES

SPEC. NO.	TEMPERATURE °C	°F	STRENGTH [KSI]	[MPa]	LONGITUDINAL STIFFNESS[a] [10^6psi]	[GPa]
A. $[0°]_8$						
1380/4/10X	21	70	166.8	1150	28.7	198[b] (ν_{LT} = 0.29)
1384/5/2			169.6	1169	29.9	206
1382/1/9			172.0	1186	27.3	188
1383/5/1			172.2	1187	28.7	198
1381/4/11			175.9	1213	27.3	188
1401/3/9			178.0	1227	28.6	197
1399/2/7			182.2	1256	30.9	213
1380/2/7			186.5	1286	28.3	195
1401/1/9			187.8	1295	-	-
1399/2/1X			198.1	1304	29.0	200
1401/4/9			193.5	1334	28.1	194
1401/3/3			197.8	1364	30.6	211[b] (ν_{LT} = 0.23)
1401/4/7			198.6	1369	-	-
1399/1/1			199.7	1377	28.9	199
1384/3/1			201.2	1387	27.4	189
1382/3/4			204.9	1413	28.3	195
1382/5/11X			206.3	1422	29.3	202
1399/1/9			213.8	1475	-	-
1379/2/3			224.1	1545	27.1	187
1380/5/3	93	200	109.7	756	38.3	264[b]
1381/4/1			130.5	900	30.9	213[b]
1382/5/7	204	400	206.4	1423	36.4	251[b]/231[c]
1378/1/9			237.9	1640	35.0	241[b]/256[c]
1399/4/6			242.5	1672	28.1	194[b]/193[c] (ν_{LT}=0.23)[c]
B. $[90°]_8$						
1384/2/4	21	70	13.8	95	21.0	145
1384/1/2A			16.1	111	18.4	127
1383/1/7A			15.8	109	17.0	117[b] (ν_{LT} = 0.129)
1380/5/2			13.9	96	23.2	160
1384/1/12			16.7	115	20.3	140
1383/1/1			15.5	107	17.7	122
1384/1/2B	204	400	12.0	83	14.8	102[b]
1384/2/12			12.6	87	16.8	116[b]
1382/4/2	316	600	5.1	35	-	-

a. Extensometer data, strain gage data not shown here.

b. Strain gage data.

c. Room temperature values.

TABLE II: STRENGTH AND STIFFNESSES OF UNNOTCHED BORON ALUMINUM 8.0 MIL 1100F AT ROOM AND ELEVATED TEMPERATURES

SPEC. NO.	TEMPERATURE °C	°F	LONGITUDINAL STIFFNESS[(a)] [10^6 psi]	[GPa]	POISSON'S RATIO	STRENGTH [ksi]	[MPa]
1390/1/6	21	70	31.5	217	0.209	117.5	810
1390/2/4			31.2	215	-	117.7	811
1390/3/6			35.8	247	0.238	-	-
1390/3/12			22.3	154	0.224	118	814
1391/1/1			31.3	216	0.234	-	-
1391/1/2			32.2	222	0.246	-	-
1391/1/8			28.4	196	0.221	121	832
1390/1/8	93	200	34.1	235	0.217	129	891
1390/2/8			42.4	292	0.229	142	976
1390/3/6	204	400	36.8	254	0.236	123	851
1391/1/2			34.2	236	-	126	866
1391/1/1	316	600	32.3	223	0.238	121	836

a. Strain gage data
All data measured with strain gages and extensometer.

TABLE III: STRENGTH DATA AND AMPLITUDE OF ACOUSTIC EMISSION EVENTS FOR SINGLE BORON FIBERS

5.6 MIL BORON FIBERS

TEST NO.	STRENGTH [KSI]	STRENGTH [MPa]	AMPLITUDE [dB]
1	310.37	2140	96
2	336.99	2324	96
3	362.07	2497	96
4	367.55	2535	95
5	374.88	2584	96
6	376.96	2600	96
7	386.84	2667	95
8	438.68	3024	96
9	438.97	3027	95
10	470.22	3243	95
11	472.59	3259	95
12	472.59	3259	95
13	500.78	3454	96
14	518.07	3572	95
15	525.86	3627	96
16	526.24	3629	95
17	542.37	3739	38
18	569.89	3930	-
19	572.88	3951	95
AVG.	450.78	3108	
S.D.	81.78	563	

8.0 MIL BORON FIBERS

TEST NO.	STRENGTH [KSI]	STRENGTH [MPa]	AMPLITUDE [dB]
1	209.11	1442	98
2	248.69	1715	98
3	320.30	2208	98
4	346.82	2391	98
5	356.00	2454	98
6	366.05	2524	98
7	441.89	3047	98
8	443.52	3058	98
9	450.66	3107	98
10	473.10	3262	98
11	488.72	3369	98
12	490.13	3379	98
13	503.50	3471	98
14	522.97	3606	98
15	546.95	3771	98
16	564.29	3891	98
17	578.51	3989	98
AVG.	432.42	2981	
S.D.	134.43	926.8	

TABLE IV: LOCAL COMPLIANCE OF CENTER NOTCHED BORON ALUMINUM $[0°]_8$ AND $[90°]_8$ 5.6 MIL 6061F AT ELEVATED TEMPERATURE

$[0°]_8$ 5.6 Mil B/Al 6061F
SPEC. NO. UN-1382/6/3
NOTCH LENGTH = 12.89 mm (0.507 inch)

TEMP.	21	93	204	260	316	371	[°C]
LOAD NO.	70	200	400	500	600	700	[°F]
1	4.62	4.67	5.08	5.41	6.12	7.63	
2	4.52	4.61	5.06	5.34	5.92	6.74	
3	4.57	4.60	5.00	5.31	5.88	6.88	
Average	4.57	4.63	5.05	5.35	5.97	7.09	
S.D.	0.04	0.04	0.04	0.04	0.10	0.40	
% Change	-	1.31	10.5	17.1	30.6	55.1	

$[90°]_8$ 5.6 Mil B/Al 6061F
SPEC. NO. TN-1399/3/2
NOTCH LENGTH = 12.87 mm (0.507 inch)

TEMP.	21	93	204	260	316	371	[°C]
LOAD NO.	70	200	400	500	600	700	[°F]
1	6.10	-	6.87	7.37	7.96	8.83	
2	5.98	6.49	6.86	7.31	7.49	8.73	
3	5.88	6.31	6.87	7.14	8.03	8.54	
4	6.04	-	6.70	7.44	7.93	8.76	
5	-	-	-	7.35	7.68	8.78	
6	-	-	-	7.43	7.81	8.76	
7	-	-	-	-	-	8.62	
Average	6.00	6.40	6.74	7.34	7.82	8.72	
S.D.	0.93	0.13	0.06	0.11	0.20	0.10	
% Change	-	6.6	13.9	22.3	30.3	45.3	

TABLE V: LOCAL COMPLIANCE OF CENTER NOTCHED BORON ALUMINUM $[0°]_8$ 5.6 MIL 6061F AT ROOM AND ELEVATED TEMPERATURES

SPEC. NO.	2a/W	TEMPERATURE °C	TEMPERATURE °F	LOCAL COMPLIANCE 10^{-3} μ/N
1384/5/5	0.051	21	70	1.189
1399/4/7	0.105	21	70	1.124
1401/4/1	0.200	21	70	1.845
1381/5/1	0.196	21	70	1.691
1382/3/7	0.198	21	70	1.734
1381/4/7	0.199	93	200	1.872
1381/5/1	0.196	204	400	1.822
1401/4/1	0.200	316	600	2.345
1380/2/5	0.297	21	70	2.574
1399/1/8	0.299	21	70	3.488
1384/2/1	0.298	21	70	2.441
1380/3/3	0.297	21	70	2.557
1382/4/1	0.298	93	200	2.461
1383/5/5	0.300	93	200	2.191
1399/1/8	0.300	204	400	2.675
1380/3/3	0.297	316	600	3.151
1382/1/7	0.406	21	70	4.060
1399/4/9	0.402	21	70	3.975
1401/3/8	0.400	21	70	3.310
1378/1/5	0.404	21	70	3.512
1380/4/9	0.397	21	70	3.687
1382/1/7	0.406	93	200	4.015
1399/4/9	0.402	204	400	4.327
1401/3/8	0.401	316	600	3.870
1382/6/3	0.509	21	70	4.568
1383/5/4	0.509	21	70	4.810
1382/3/9	0.507	21	70	4.576
1399/4/5	0.508	21	70	5.090
1384/3/3	0.509	21	70	5.300
1380/4/10	0.507	21	70	5.822
1382/6/3	0.509	93	200	4.626
1383/5/4	0.509	93	200	5.477
1382/6/3	0.509	204	400	5.048
1382/3/9	0.507	204	400	5.141
1399/4/5	0.508	204	400	5.940
1382/6/3	0.509	260	500	5.355
1382/6/3	0.509	316	600	5.974
1384/3/3	0.509	316	600	6.530
1382/6/3	0.509	371	700	7.088

TABLE VI: GLOBAL COMPLIANCE OF BORON ALUMINUM $[0°]_8$ and $[90°]_8$ 5.6 MIL 6061F AT ROOM TEMPERATURE

$[0°]_8$			$[90°]_8$		
SPEC. NO.	2a/W	GLOBAL COMPLIANCE $[10^{-3}$ μ/N]	SPEC. NO.	2a/W	GLOBAL COMPLIANCE $[10^{-3}$ μ/N]
1384/5/5	0.051	3.073	1382/4/3	0.102	3.339
1399/4/8	0.051	3.311	1381/1/4	0.101	6.424*
1380/4/8	0.051	3.244			
			1378/1/10	0.300	5.465
1382/6/8	0.101	3.198	1384/2/11	0.299	6.186
1380/4/1	0.101	2.958	1380/5/3	0.298	6.118
1399/1/5	0.102	3.634	1381/1/1	0.300	9.517*
1382/3/7	0.198	3.474	1383/2/1	0.511	9.566
1379/2/9	0.200	3.541	1384/2/1	0.500	8.672
1384/5/4	0.200	5.23*			
1380/4/7	0.194	4.76*			
1380/2/5	0.297	3.85			
1381/3/7	0.302	4.12			
1382/5/2	0.303	4.33			
1401/3/8	0.401	4.47			
1378/1/5	0.404	5.39			
1380/3/7	0.403	4.08			
1380/4/10	0.507	4.81			
1381/3/8	0.508	4.61			

* Data not reliable

TABLE VII: NOTCHED STRENGTH OF BORON ALUMINUM 5.6 MIL 6061F $[0°]_8$ AT ROOM AND ELEVATED TEMPERATURES

SPEC. No.	2a/W(1)	Y σ_f/σ_o (2)
A. 21°C (70°F)		
1384/5/5	0.051	0.730
1399/4/8	0.051	0.931
1381/3/10	0.052	0.932
		0.864
1382/6/8	0.100	0.780
1380/4/1	0.101	0.669
1399/4/7	0.105	0.858
1380/3/10	0.102	0.865
1399/1/5	0.102	0.838
		0.802
1382/3/7	0.198	0.685
1379/2/9	0.200	0.766
1380/3/4	0.199	0.698
		0.716
1380/2/5	0.297	0.572
1381/3/7	0.302	0.582
1384/5/1	0.301	0.411
1381/1/2	0.299	0.632
1399/4/3	0.304	0.599
1382/5/2	0.303	0.578
		0.562
1371/1/5	0.403	0.526
1380/3/7	0.403	0.548
1380/4/9	0.397	0.481
1399/1/7	0.401	0.564
1381/3/1	0.403	0.547
1382/3/1	0.401	0.489
1382/5/8	0.421	0.523
1383/6/1	0.402	0.556
		0.526
1380/4/10	0.507	0.496
1381/3/8	0.505	0.455
1380/3/8	0.508	0.496
1399/1/6	0.507	0.489
1382/5/6	0.507	0.442
1380/4/6	0.509	0.480
1382/4/2	0.505	0.503
		0.480
B. 93°C (200°F)		
1381/4/7	0.199	0.711
1382/4/7	0.298	0.648
1382/1/7	0.406	0.514
1383/5/4	0.509	0.520
C. 204°C (400°F)		
1381/5/1	0.196	0.696
1399/1/8	0.299	0.650
1399/4/9	0.402	0.556
1382/3/9	0.507	0.476
1399/4/5	0.508	0.474
D. 316°C (600°F)		
1381/3/4	0.052	0.907
1380/2/1	0.055	0.816
		0.862
1382/5/10	0.100	0.789
1401/4/3	0.101	0.774
		0.782
1401/4/1	0.200	0.634
1399/2/8	0.199	0.618
1384/3/4	0.203	0.721
		0.658
1380/3/3	0.297	0.610
1382/5/5	0.301	0.586
1378/1/3	0.300	0.754
		0.650
1401/3/8	0.401	0.505
1380/4/2	0.402	0.544
1382/6/2	0.408	0.623
		0.557
1384/3/3	0.509	0.504
1381/3/3	0.506	0.497
1382/1/2	0.506	0.431
1382/6/3	0.509	0.492
		0.481

1. a ... half notch length
   W ... specimen width
2. σ_o ... unnotched strength
   σ_f ... notched strength
   Y ... isotropic width correction factor

TABLE VIII: NOTCHED STRENGTH OF BORON ALUMINUM 5.6 MIL 6061F $[90°]_8$ AT ROOM AND ELEVATED TEMPERATURES

2a/W	TEMPERATURE PC	°F	NOTCHED STRENGTH [KSI]	[MPa]
0.10	21	70	12.78	88.1
	204	400	8.89	61.3
	316	600	5.93	40.9
0.30	21	70	11.66	80.4
	204	400	8.30	57.2
	316	600	4.87	33.6
0.50	21	70	7.86	54.2
	204	400	6.11	42.1
	316	600	3.02	20.8

TABLE IX: FRACTURE DATA FOR BORON ALUMINUM 5.6 MIL 6061F LAMINATES

SPEC. NO.	LAMINATE TYPE	2a/W	GLOBAL COMPLIANCE 10^{-3} μ/N	STRENGTH [KSI]	[MPa]
1385/5/7	$[\pm 45]_{2s}$	0.202	8.248	16.46	113.5
1394/5/9	$[0/90]_{2s}$	0.054	3.670	73.41	506.1
1374/4B/1		0.104	4.28	75.87	523.1
1394/4A/3		0.200	-	41.15	311.3
1394/5/1		0.305	4.76	39.25	270.6
1394/4B/3		0.405	5.95	29.91	206.2
1394/5/3		0.502	7.99	31.20	215.1
1521/48	$[0_2/\pm 45]_s$	0.201	5.05	64.65	445.7
1524/22	$[0/\pm 45/90]_s$	0.201	5.504	40.32	278.0

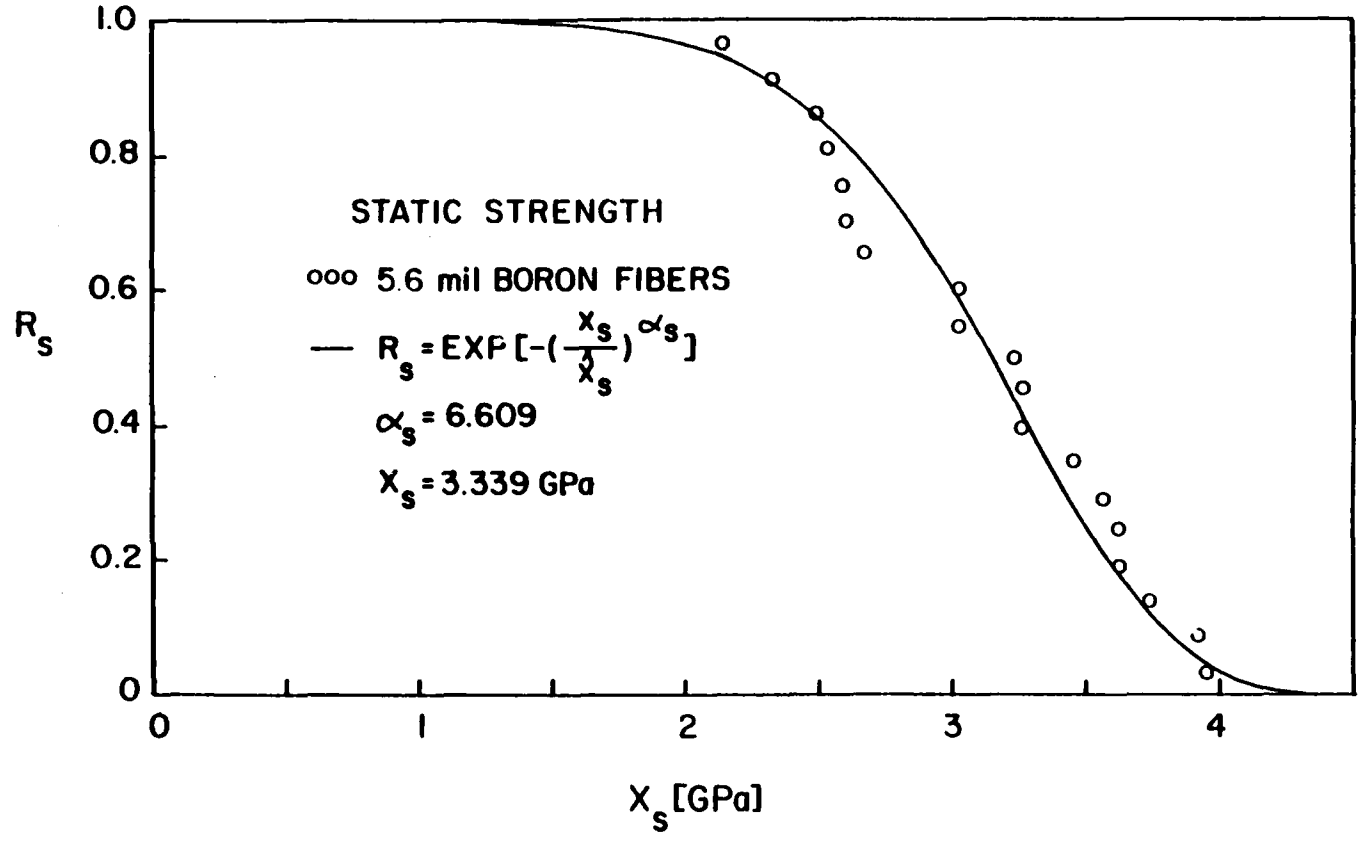

Figure 1a. Static strength distribution of individual 5.6 mil diameter boron fibers.

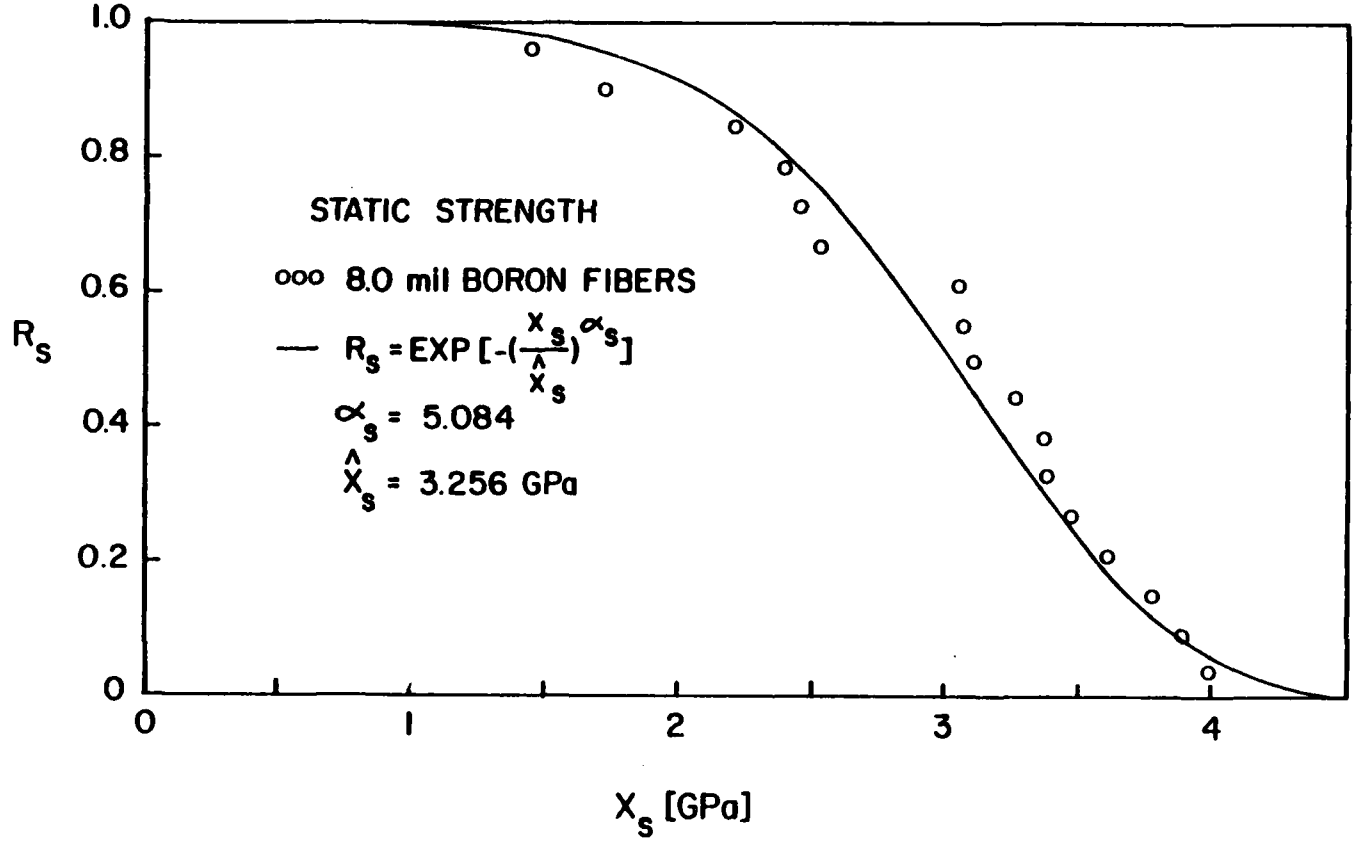

Figure 1b. Static strength distribution of individual 8.0 mil diameter boron fibers.

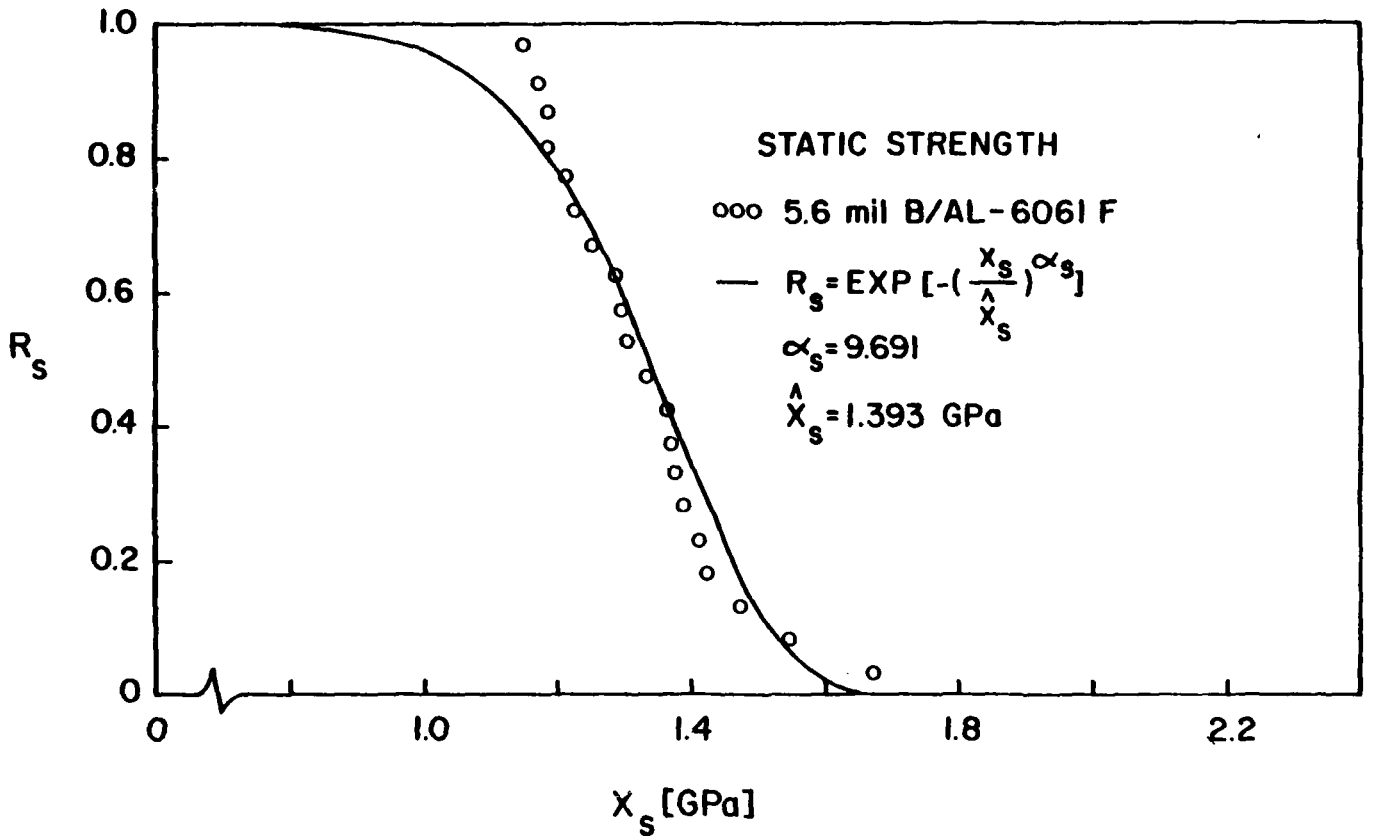

Figure 2a. Static strength distribution of unidirectional 5.6 mil B/Al-6061F

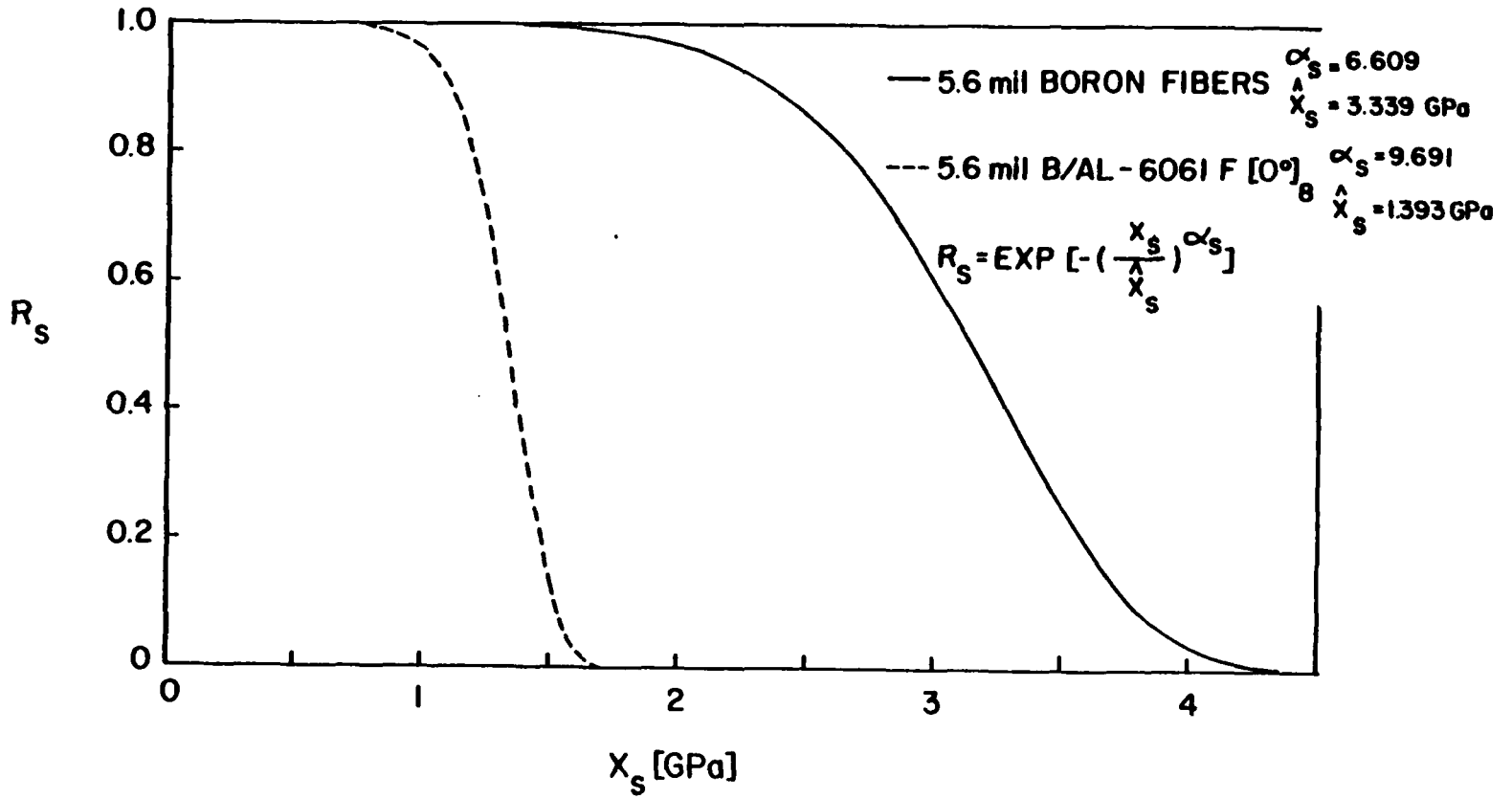

Figure 2b. Comparison between static strength distributions of unidirectional 5.6 mil B/Al-6061F specimens and 5.6 mil diameter boron fibers.

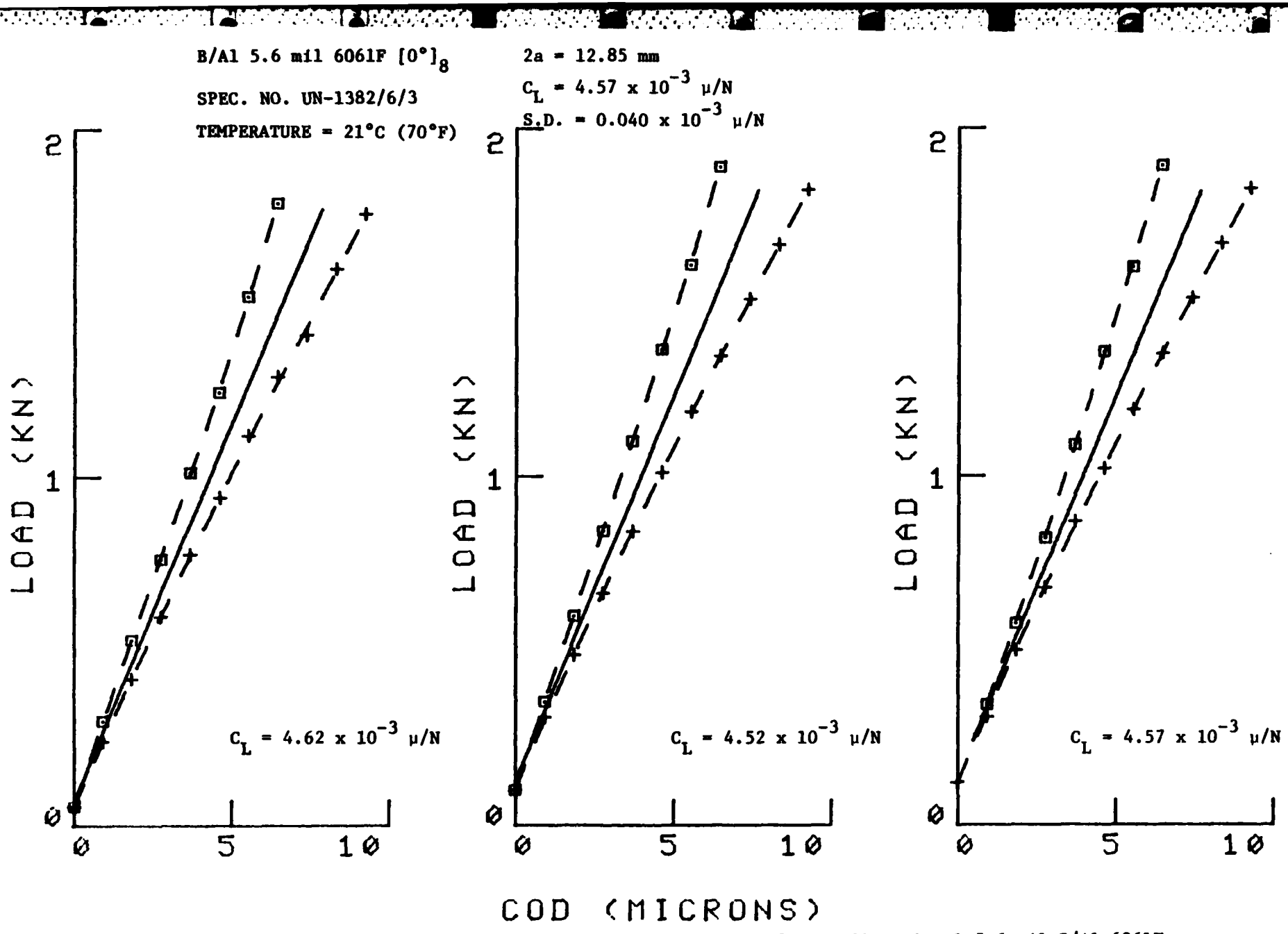

Figure 3. Example of three load-COD curves at initial loading for unidirectional 5.6 mil B/Al-6061F specimens, obtained with the IDG at room temperature.

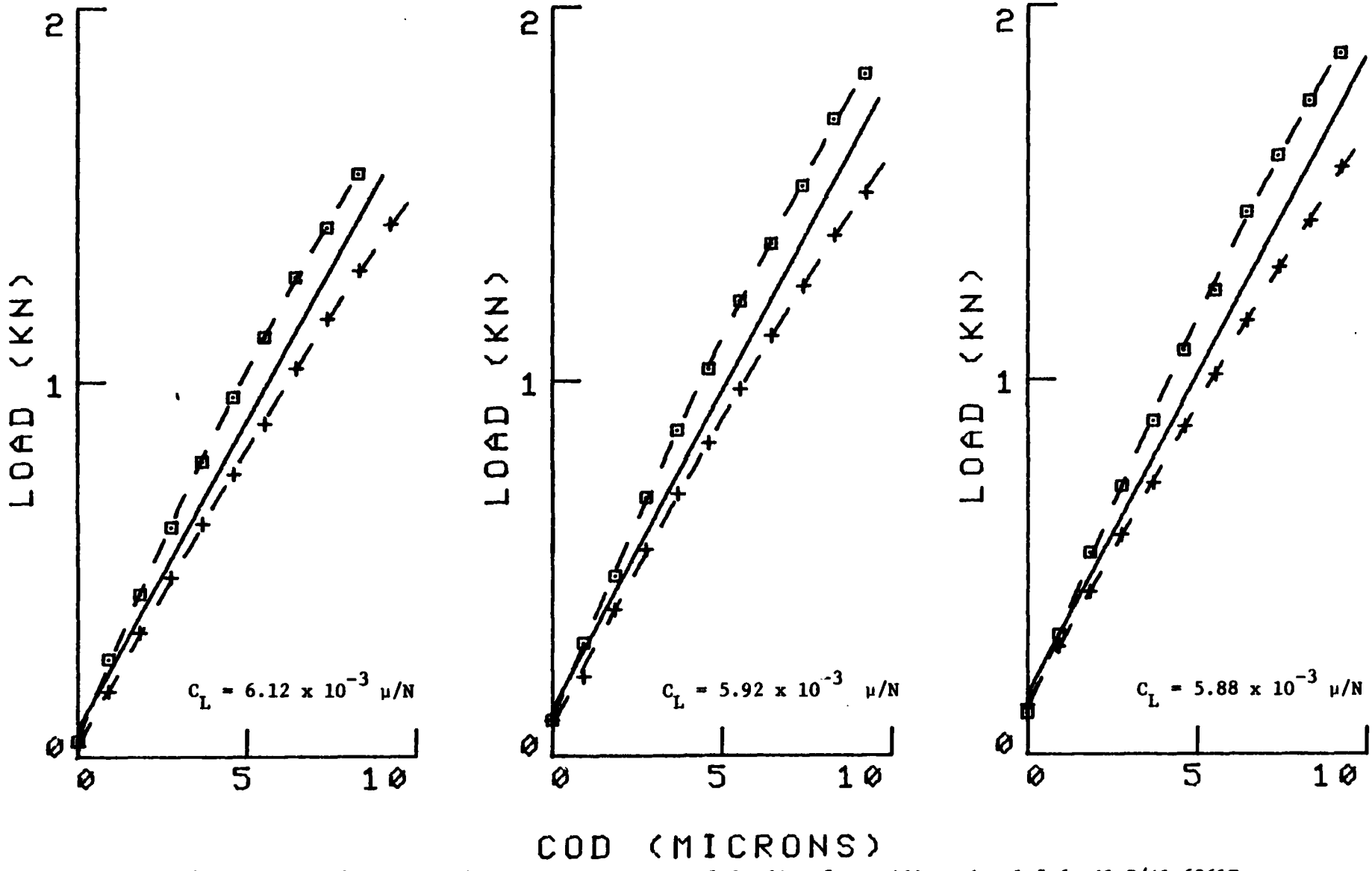

Figure 4. Example of three load-COD curves at initial loading for unidirectional 5.6 mil B/Al-6061F specimens, obtained with the IDG at 316°C.

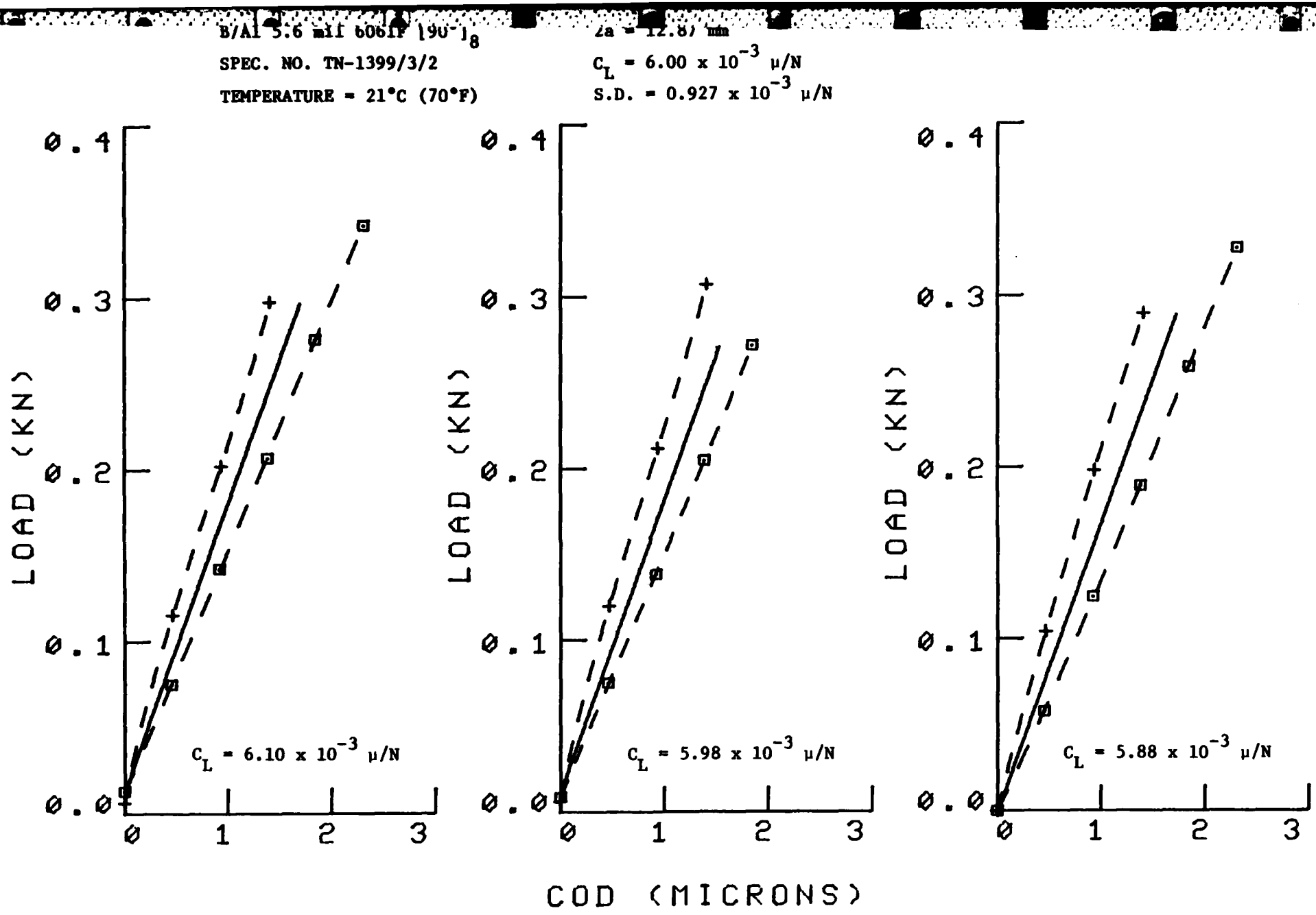

Figure 5. Example of three load-COD curves at initial loading for transverse $[90^{\circ}]_8$ 5.6 mil B/Al-6061F specimens, obtained with the IDG at room temperature.

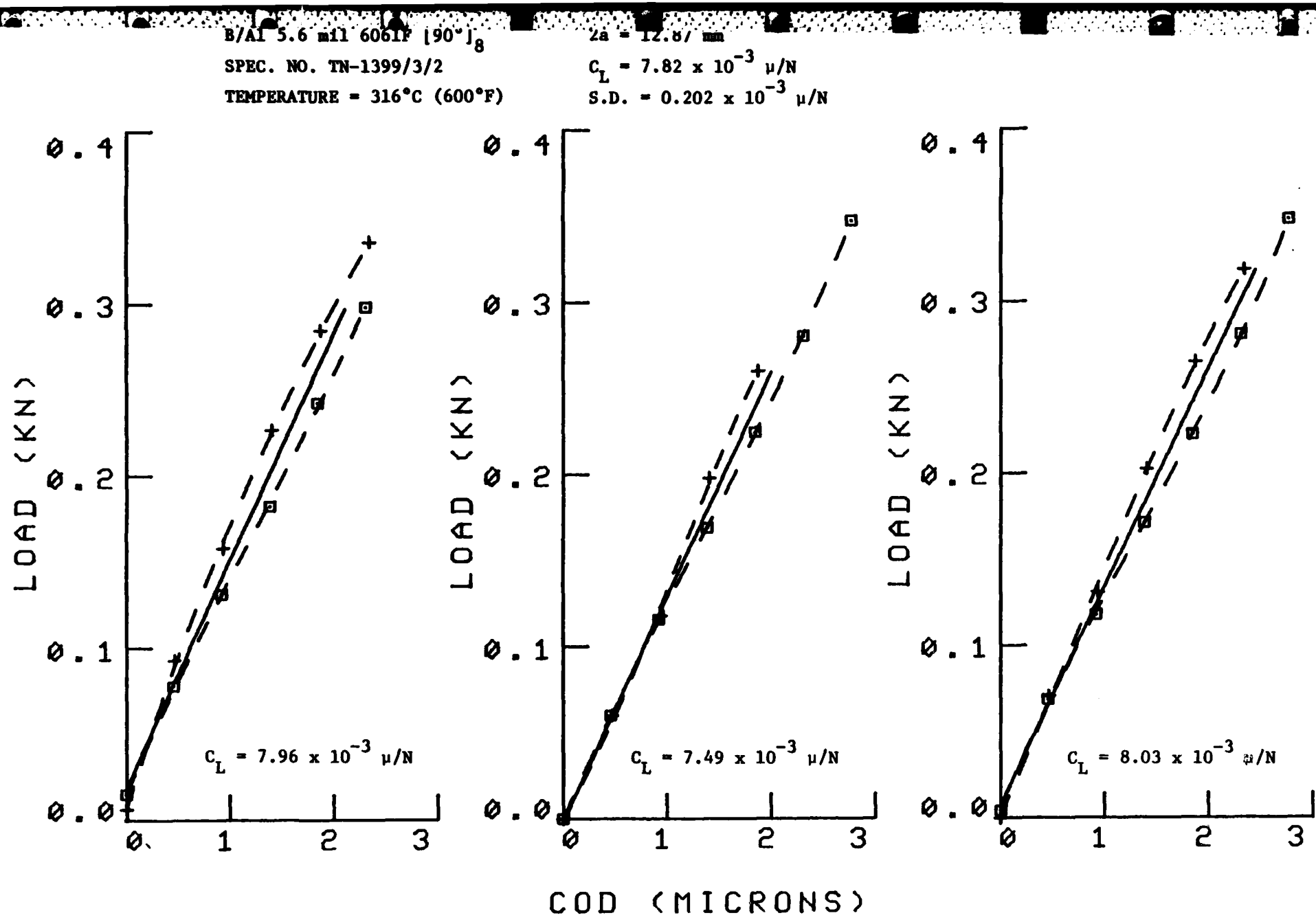

Figure 6. Example of three load-COD curves at initial loading for transverse $[90^{\circ}]_8$ 5.6 mil B/Al-6061F specimens, obtained with the IDG at 316°C

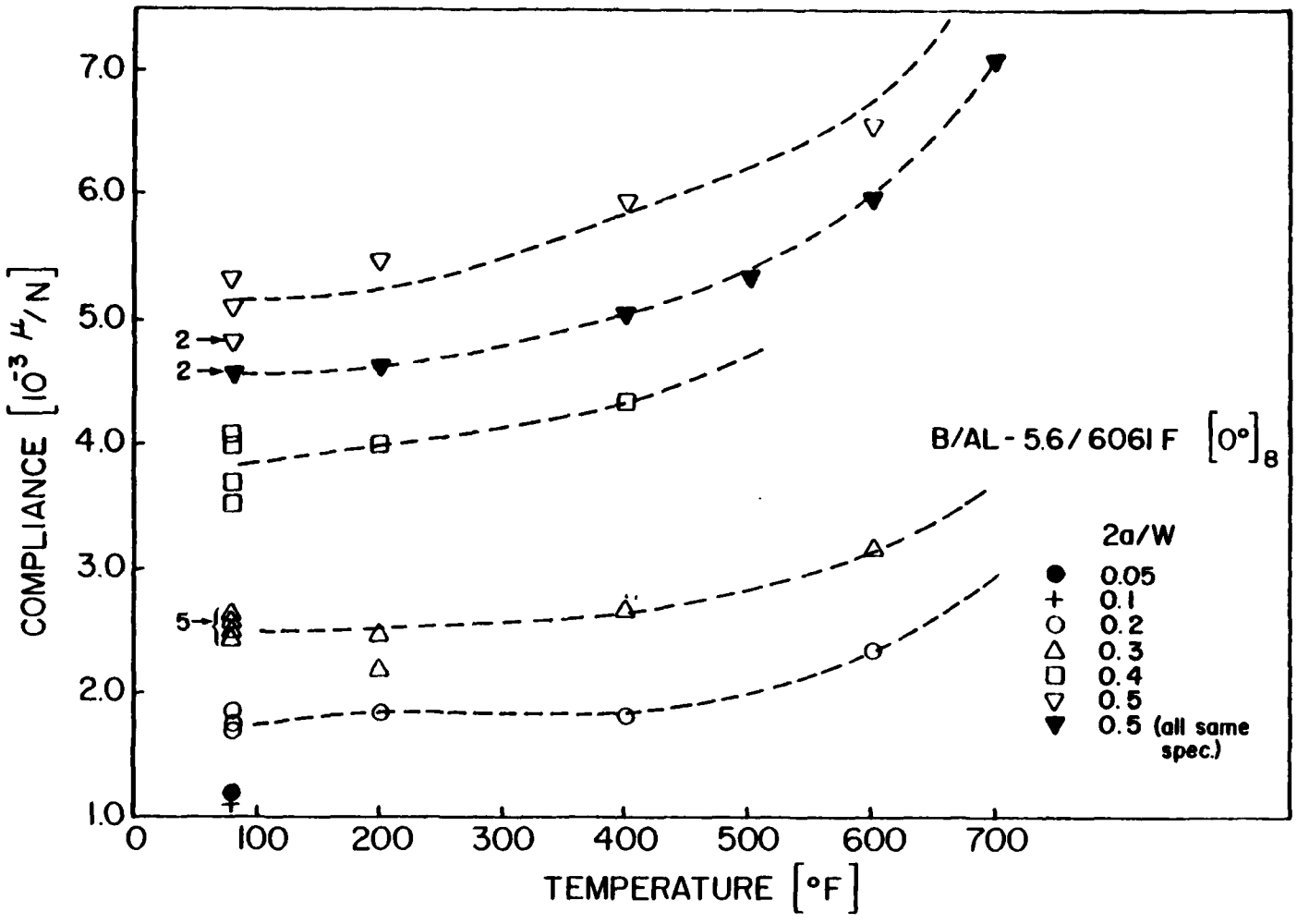

Figure 7. Local compliance versus temperature for various notch length-to-width ratios for unidirectional 5.6 mil B/Al-6061F.

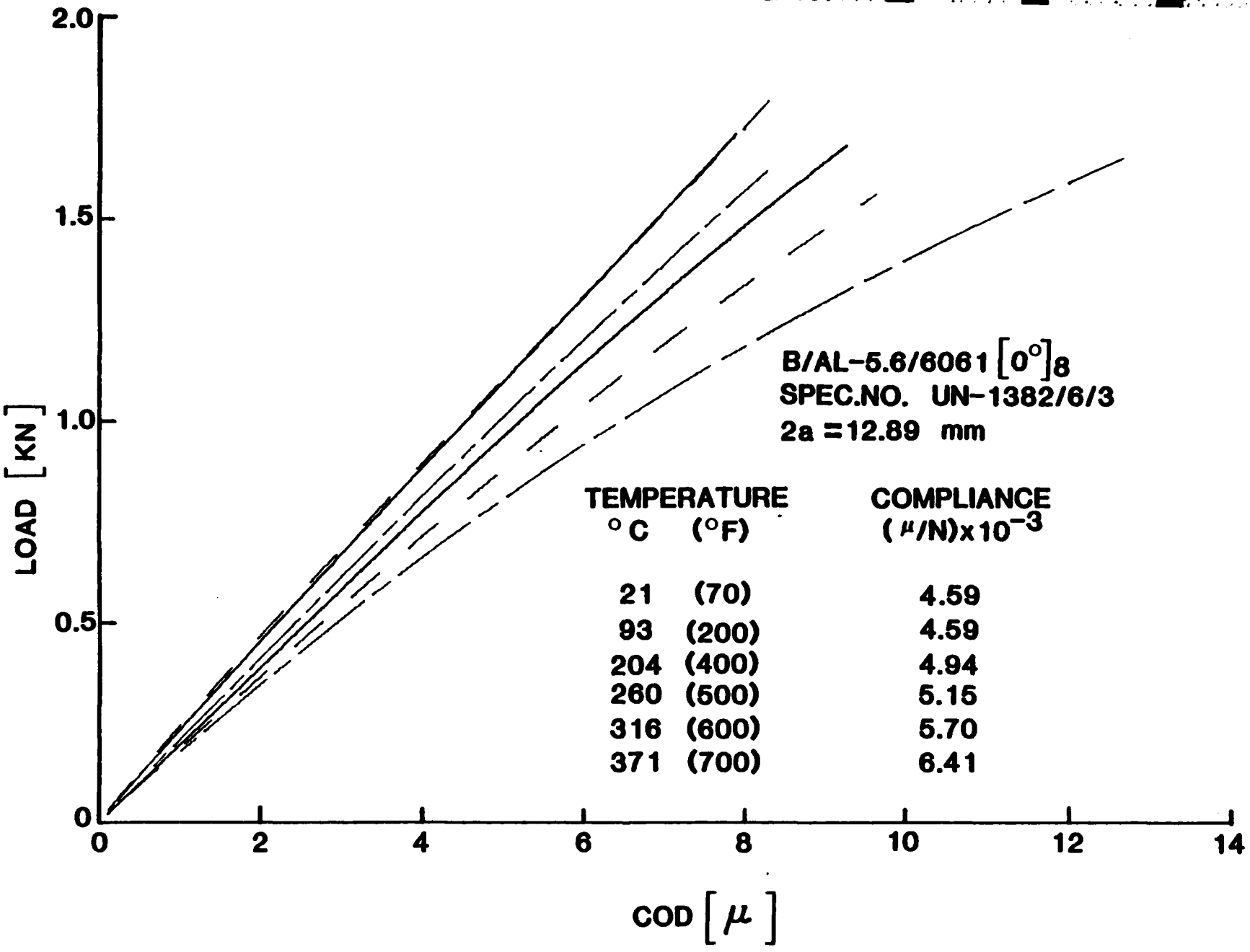

Figure 8. Initial load-COD curves for unidirectional 5.6 mil B/Al-6061F at various temperatures, obtained with the IDG.

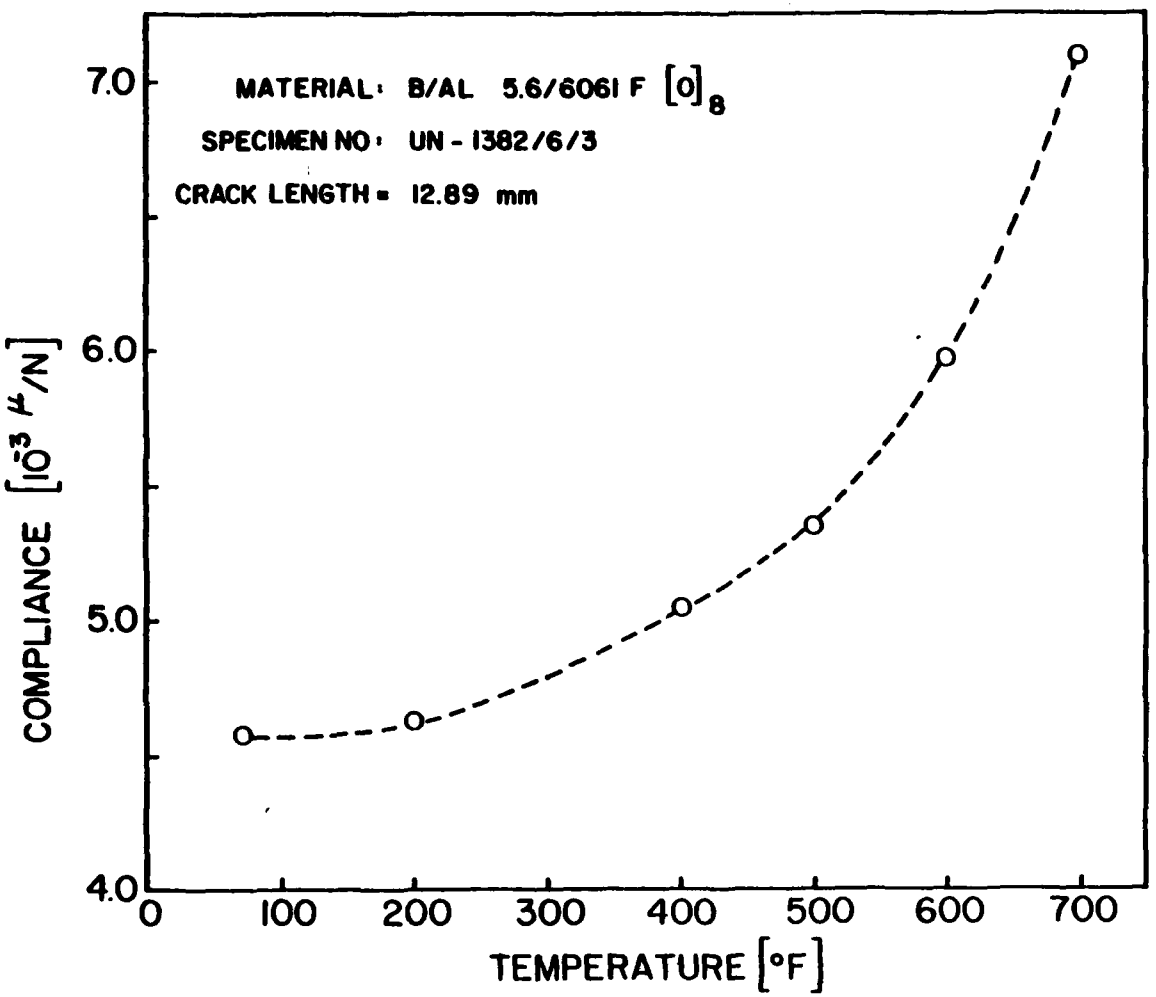

Figure 9. Local compliance versus temperature for unidirectional 5.6 mil B/Al-6061F for same specimen data shown in Figure 8.

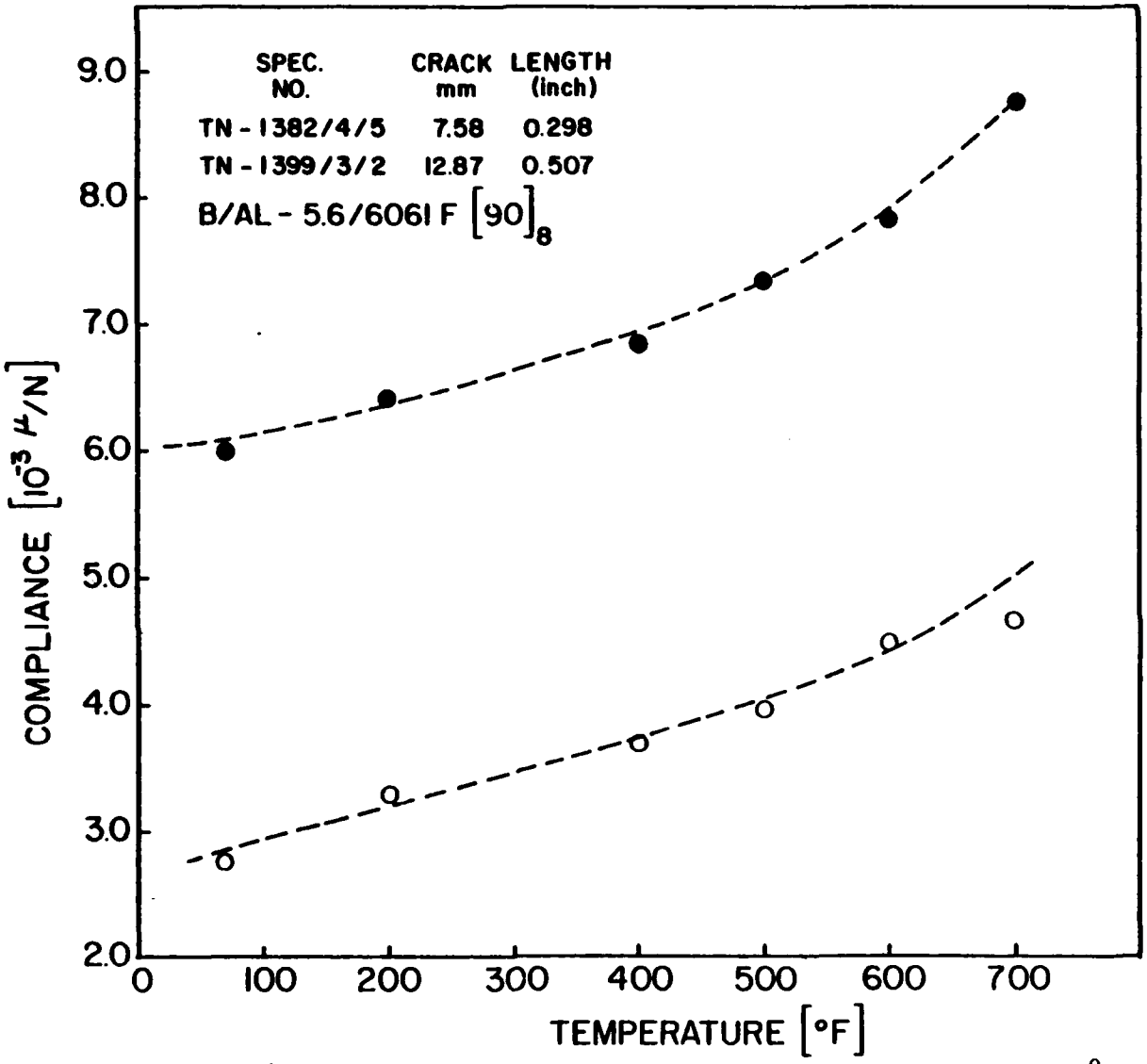

Figure 10. Local compliance versus temperature for transverse $[90^{\circ}]_8$ 5.6 mil B/Al-6061F for two different notch lengths.

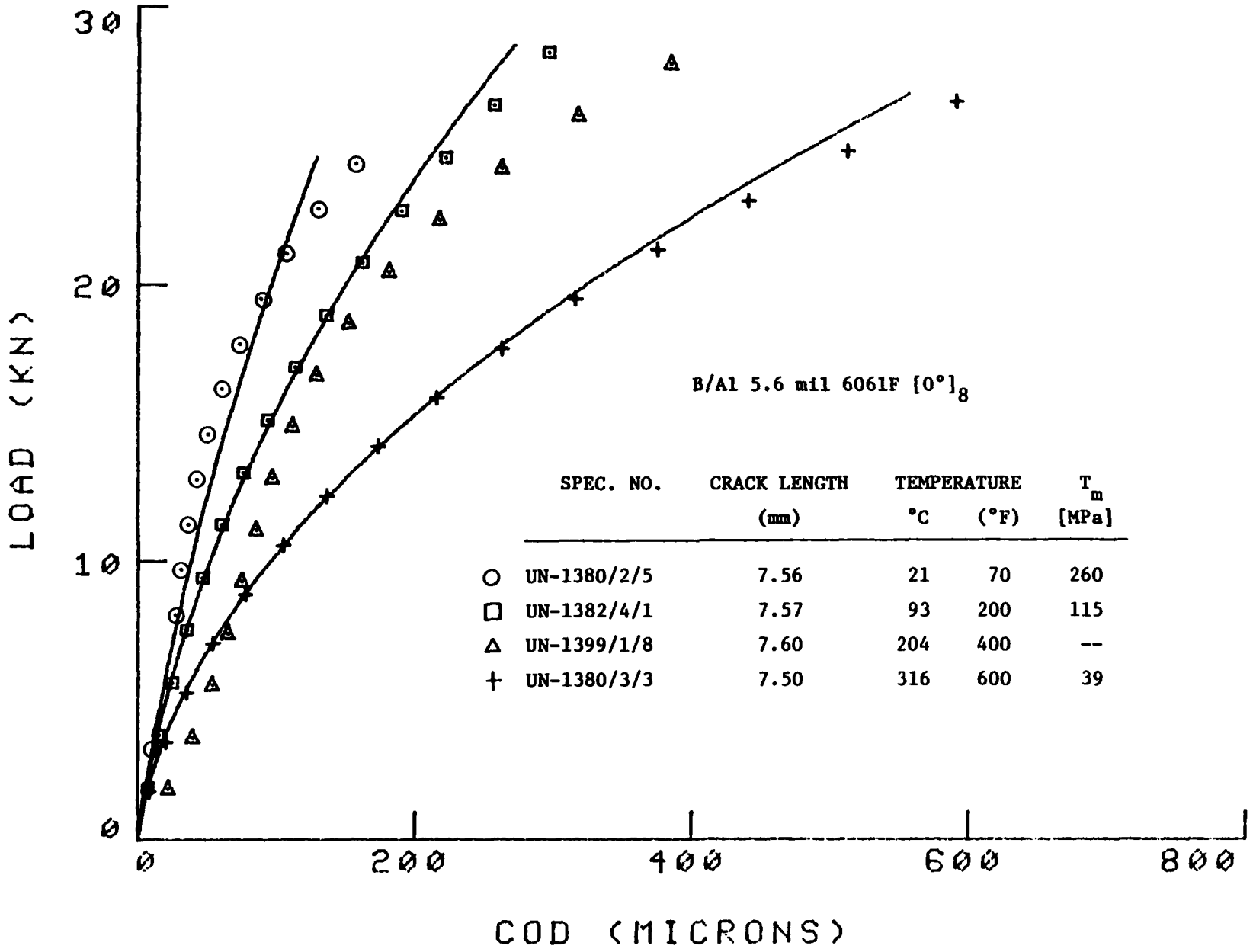

SPEC. NO.	CRACK LENGTH (mm)	TEMPERATURE °C	TEMPERATURE (°F)	T_m [MPa]
○ UN-1380/2/5	7.56	21	70	260
□ UN-1382/4/1	7.57	93	200	115
△ UN-1399/1/8	7.60	204	400	--
+ UN-1380/3/3	7.50	316	600	39

Figure 11. Load-COD curves for unidirectional 5.6 mil B/Al-6061F at various temperatures, obtained with the IDG, and comparison with analytical model [22].

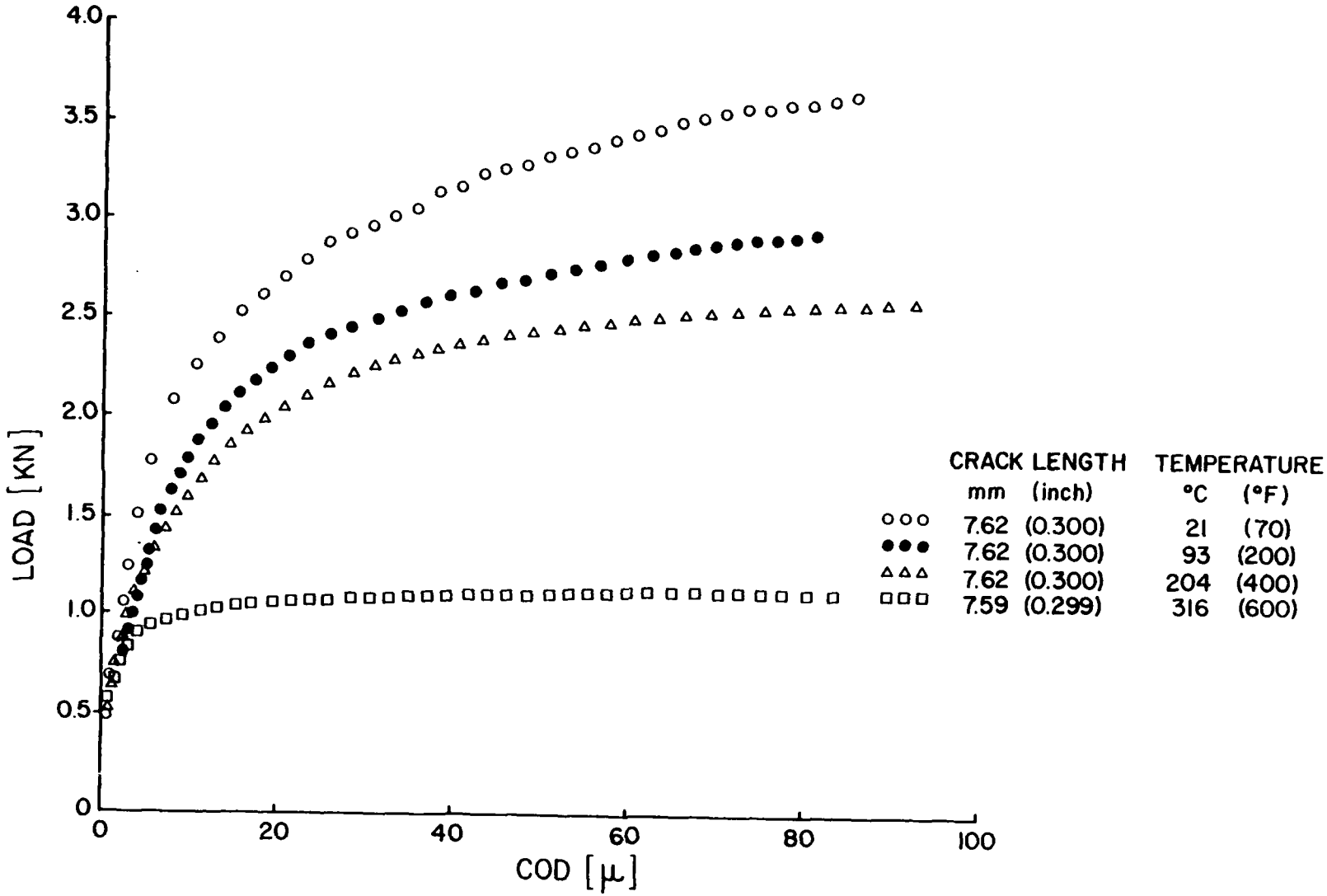

Figure 12. Load-COD curves for transverse $[90°]_8$ 5.6 mil B/Al-6061F at various temperatures, obtained with the IDG.

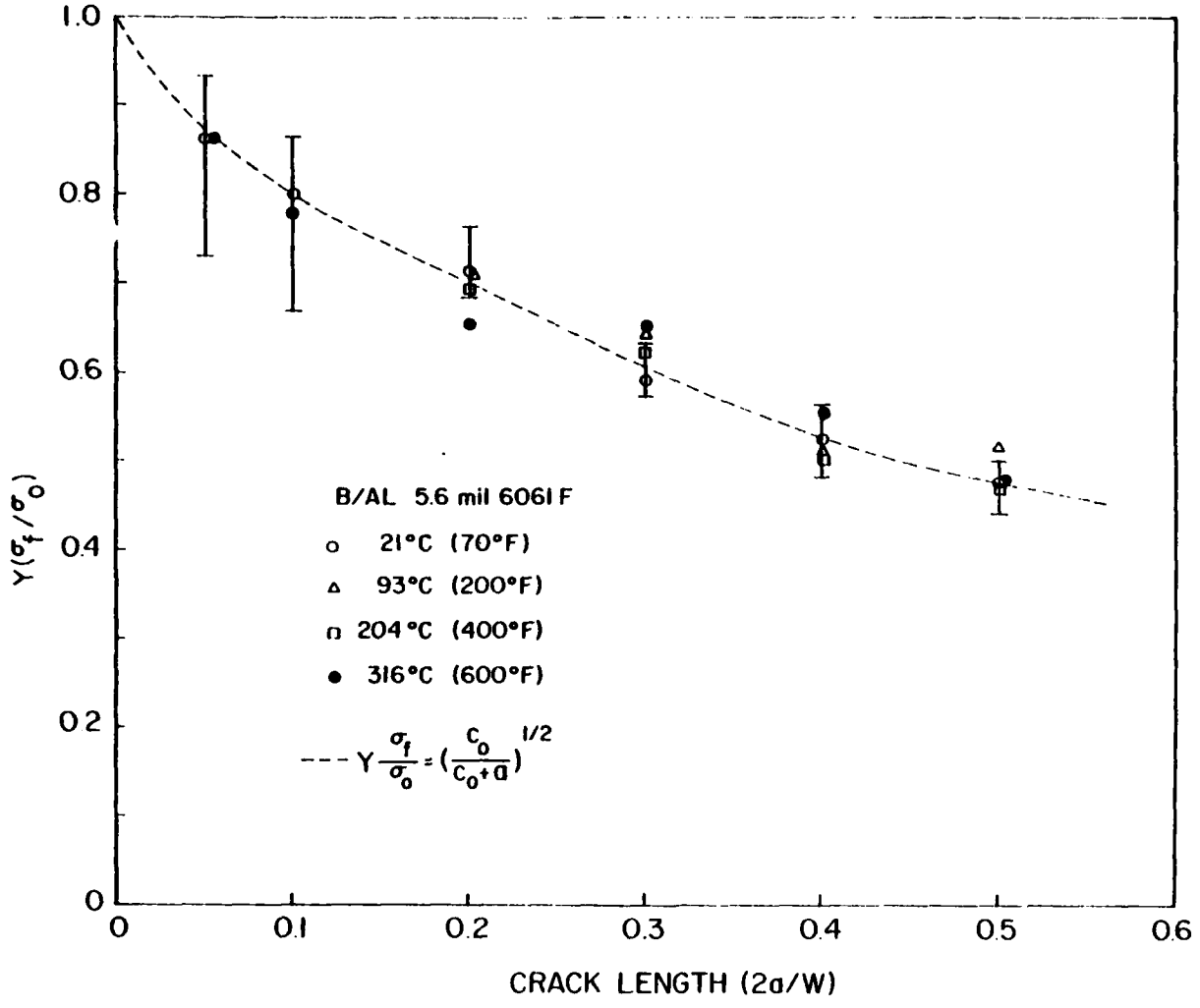

Figure 13. Notched strength at room and elevated temperatures of unidirectional 5.6 mil B/Al-6061F.

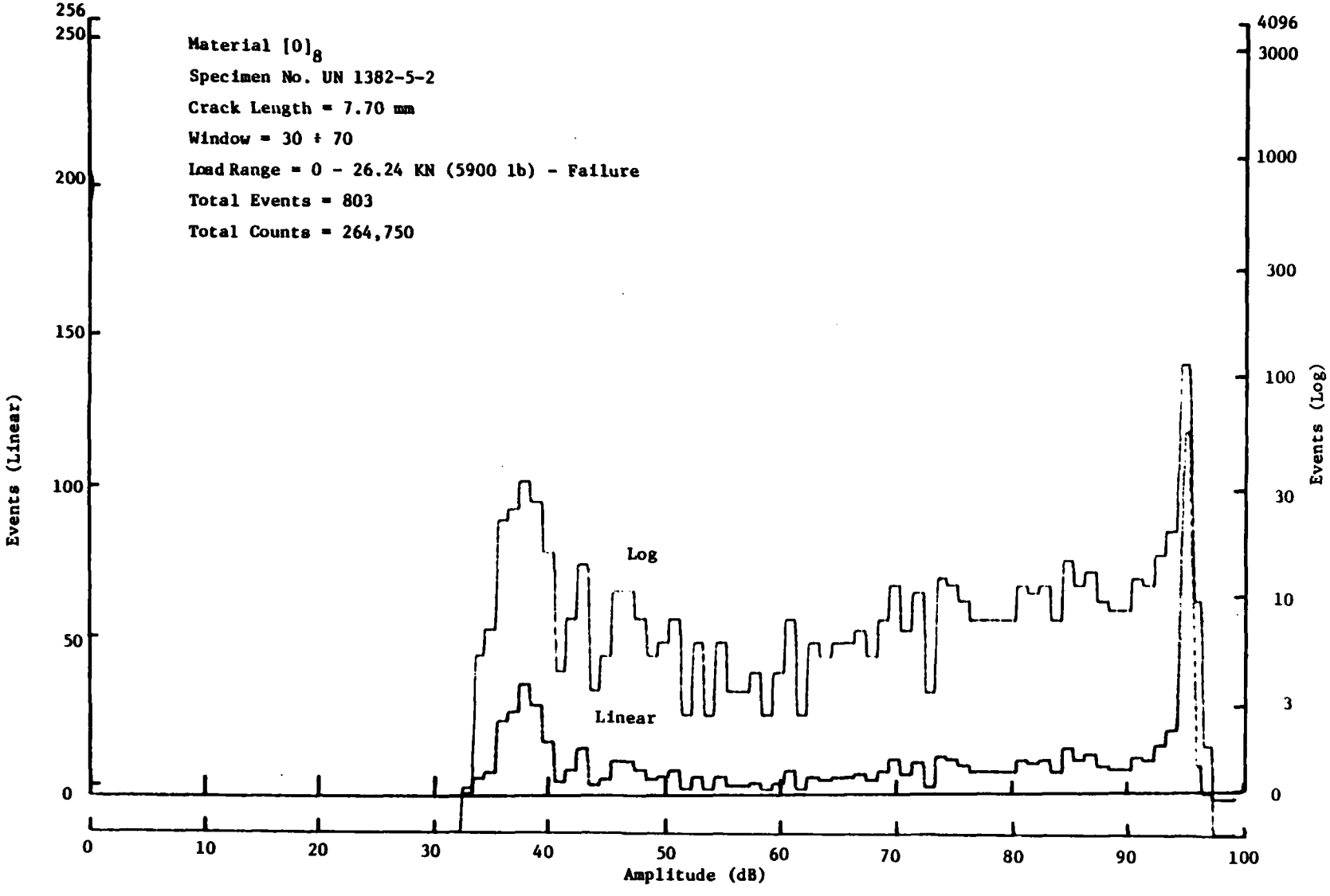

Figure 14. Amplitude distribution histograms of events (in linear and logarithmic scales) for notched unidirectional 5.6 mil B/Al-6061F after failure.

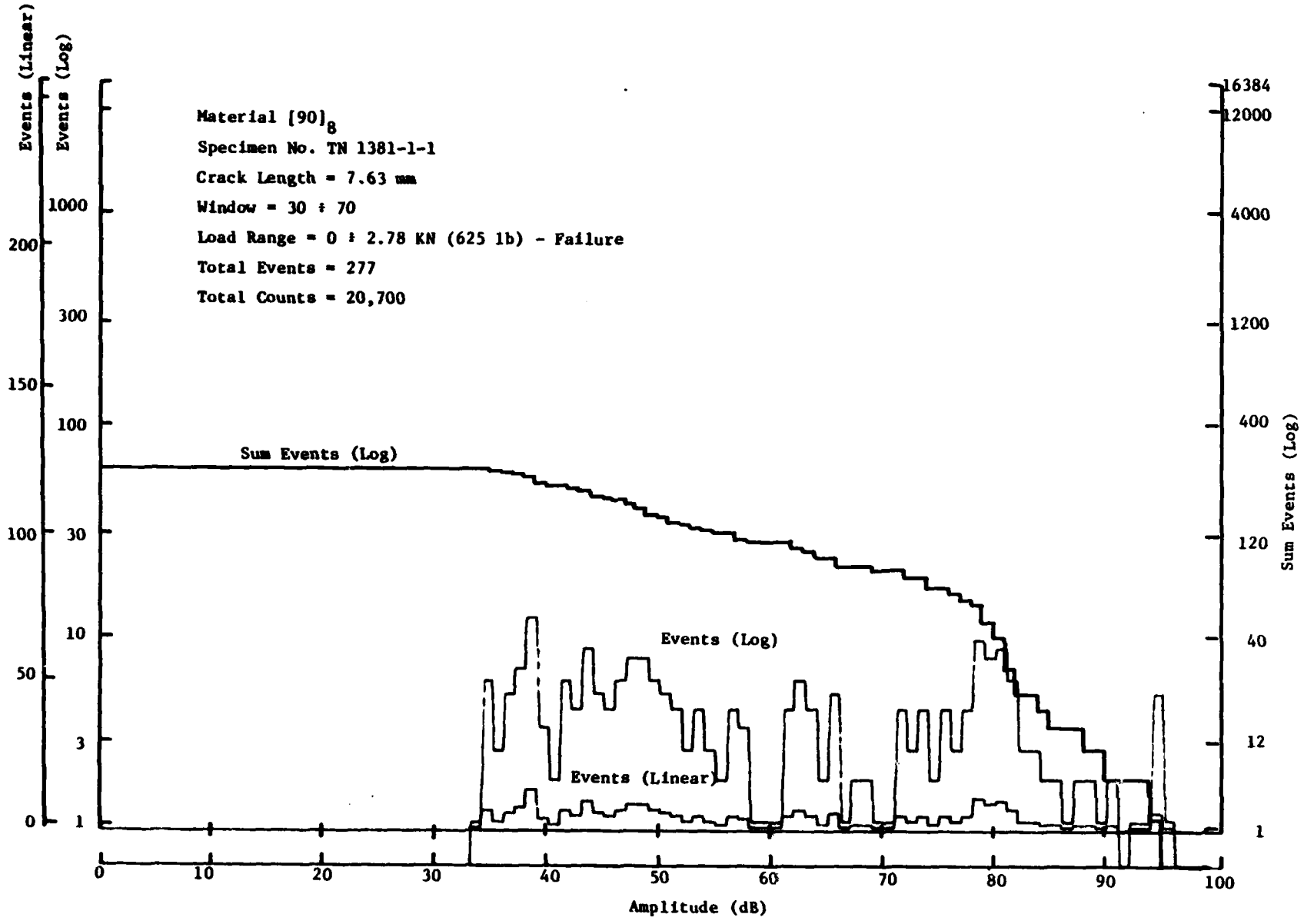

Figure 15. Amplitude distribution histograms of events (in linear and logarithmic scales) and Cumulative Event Amplitude Distribution for notched $[90°]_8$ 5.6 mil B/Al-6061F specimens after failure.

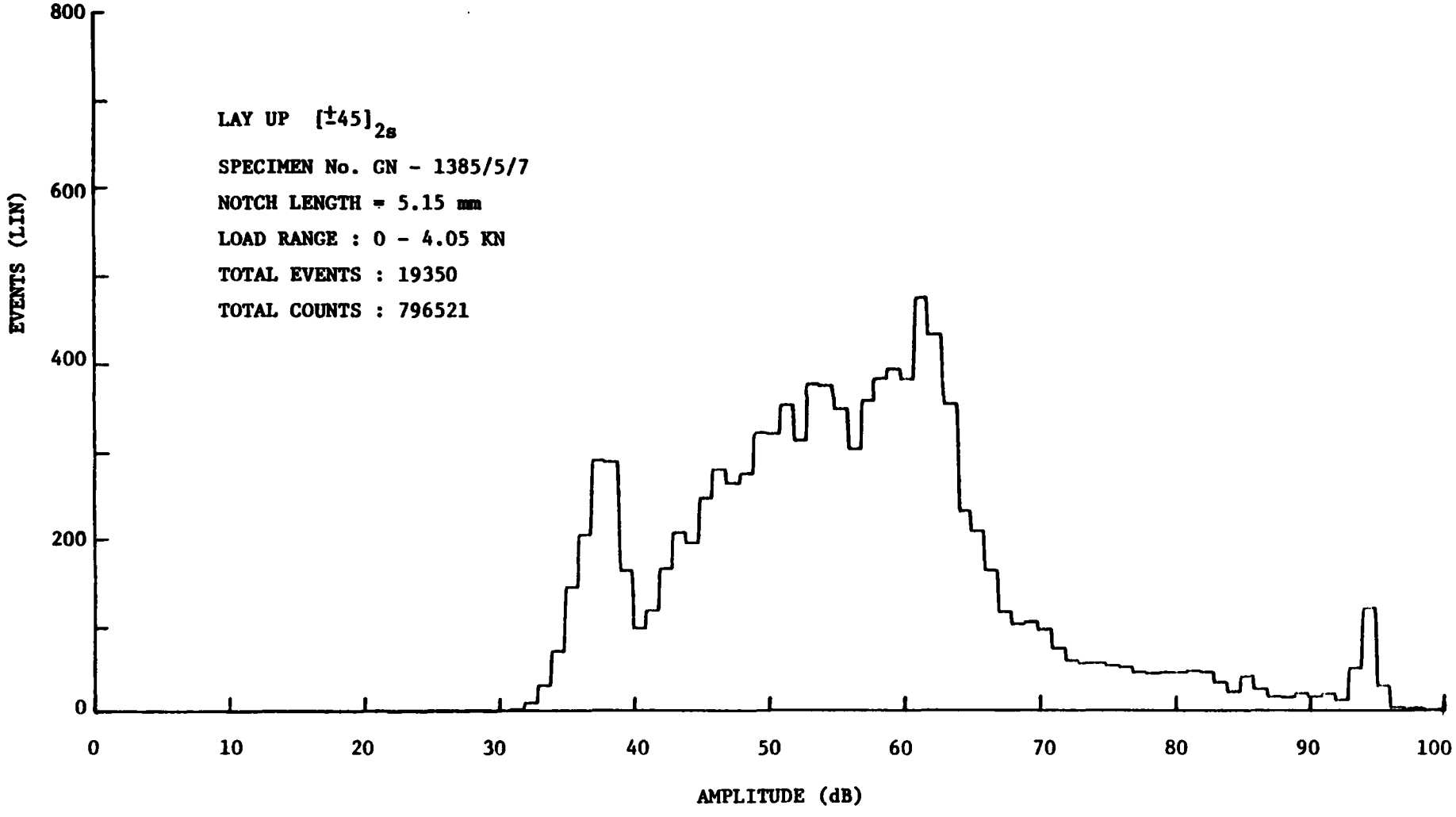

Figure 16. Amplitude distribution histogram of events for $[\pm 45]_{2s}$ 5.6 mil B/Al-6061F laminate after failure.

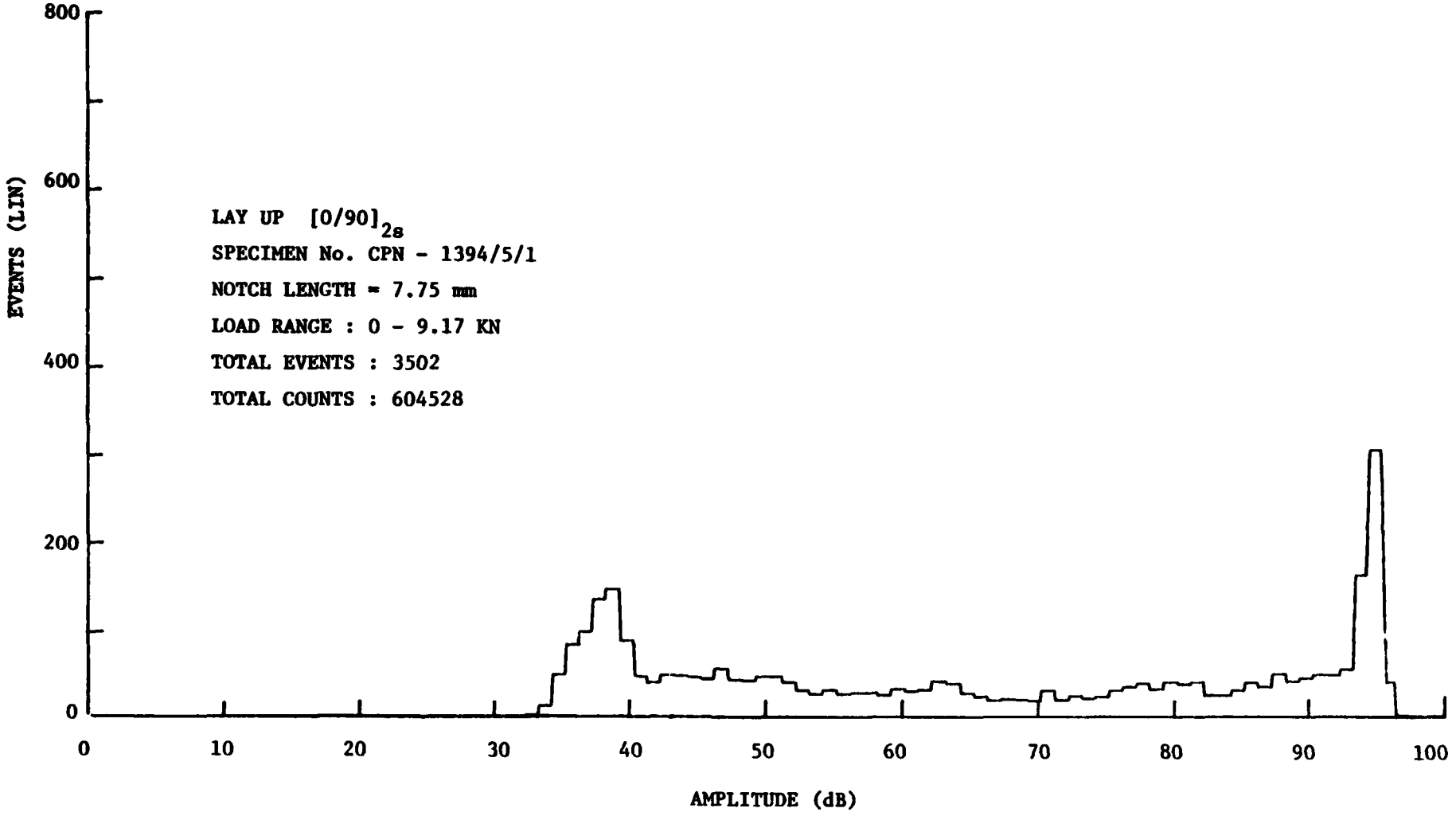

Figure 17. Amplitude distribution histogram of events for $[0/90]_{2s}$ 5.6 mil B/Al-6061F laminate after failure.

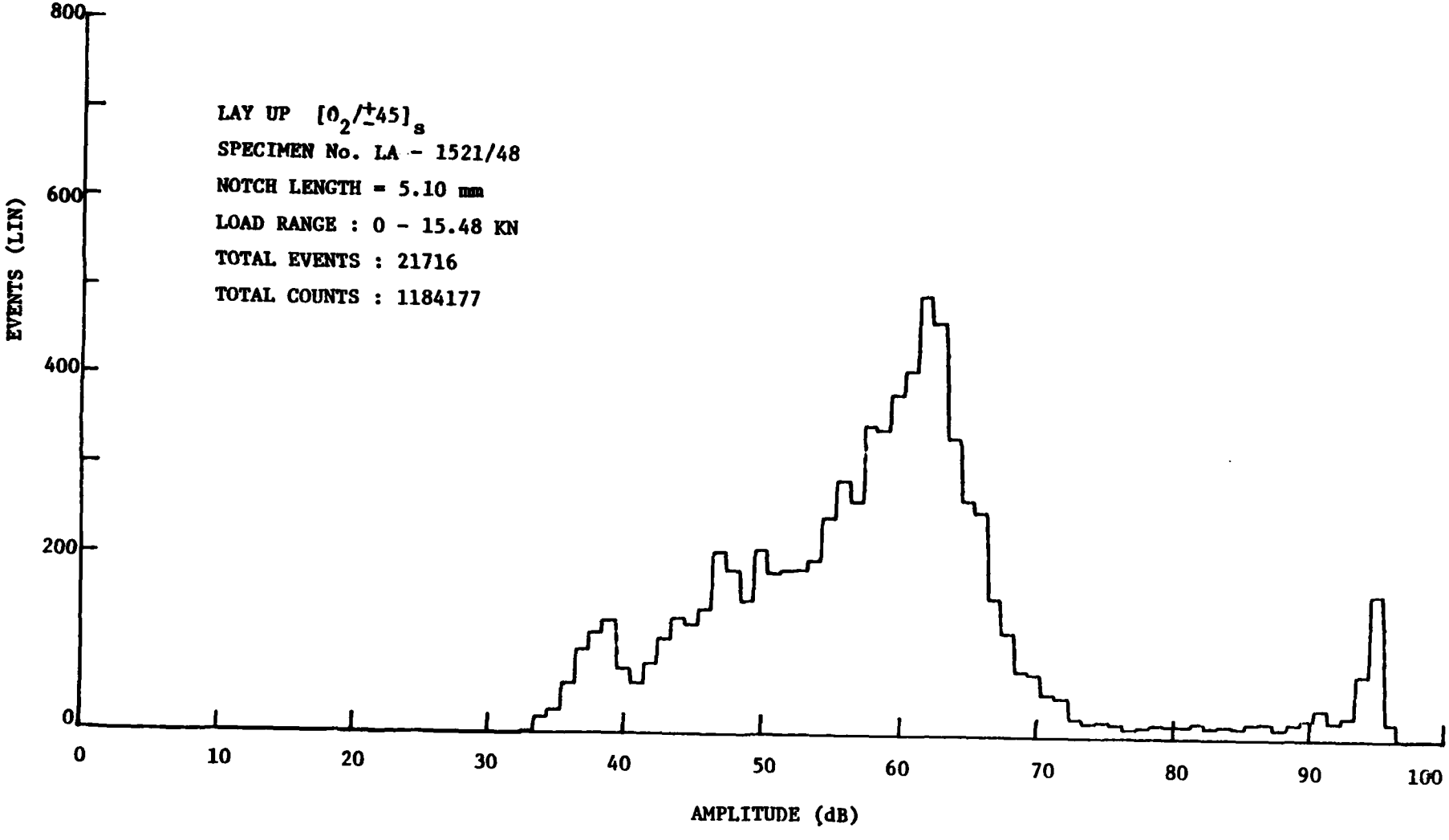

Figure 18. Amplitude distribution histogram of events for $[0_2/\pm45]_s$ 5.6 mil B/Al-6061F laminate after failure.

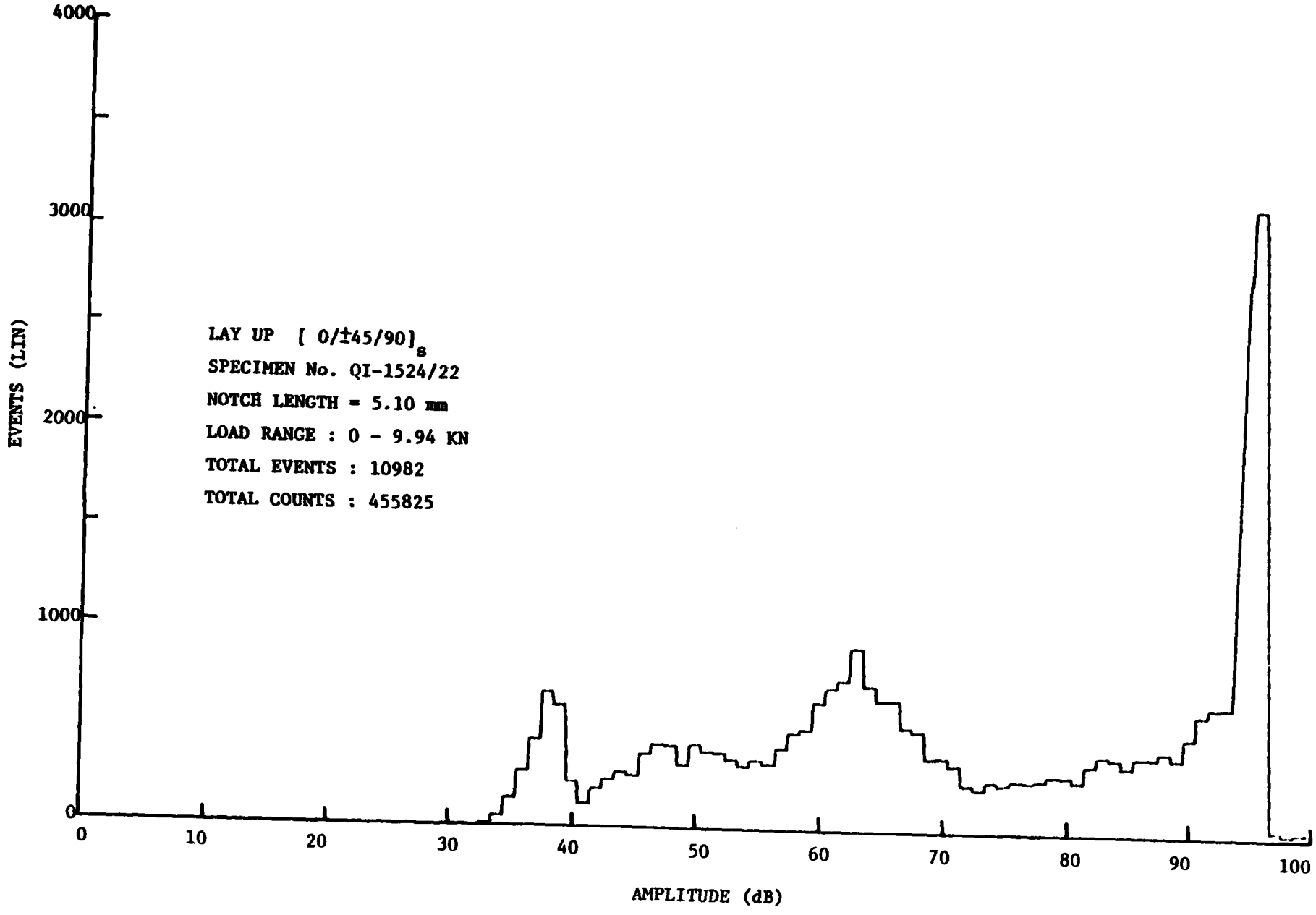

Figure 19. Amplitude distribution histogram of events for $[0/\pm45/90]_s$ 5.6 mil B/Al-6061F laminate after failure.

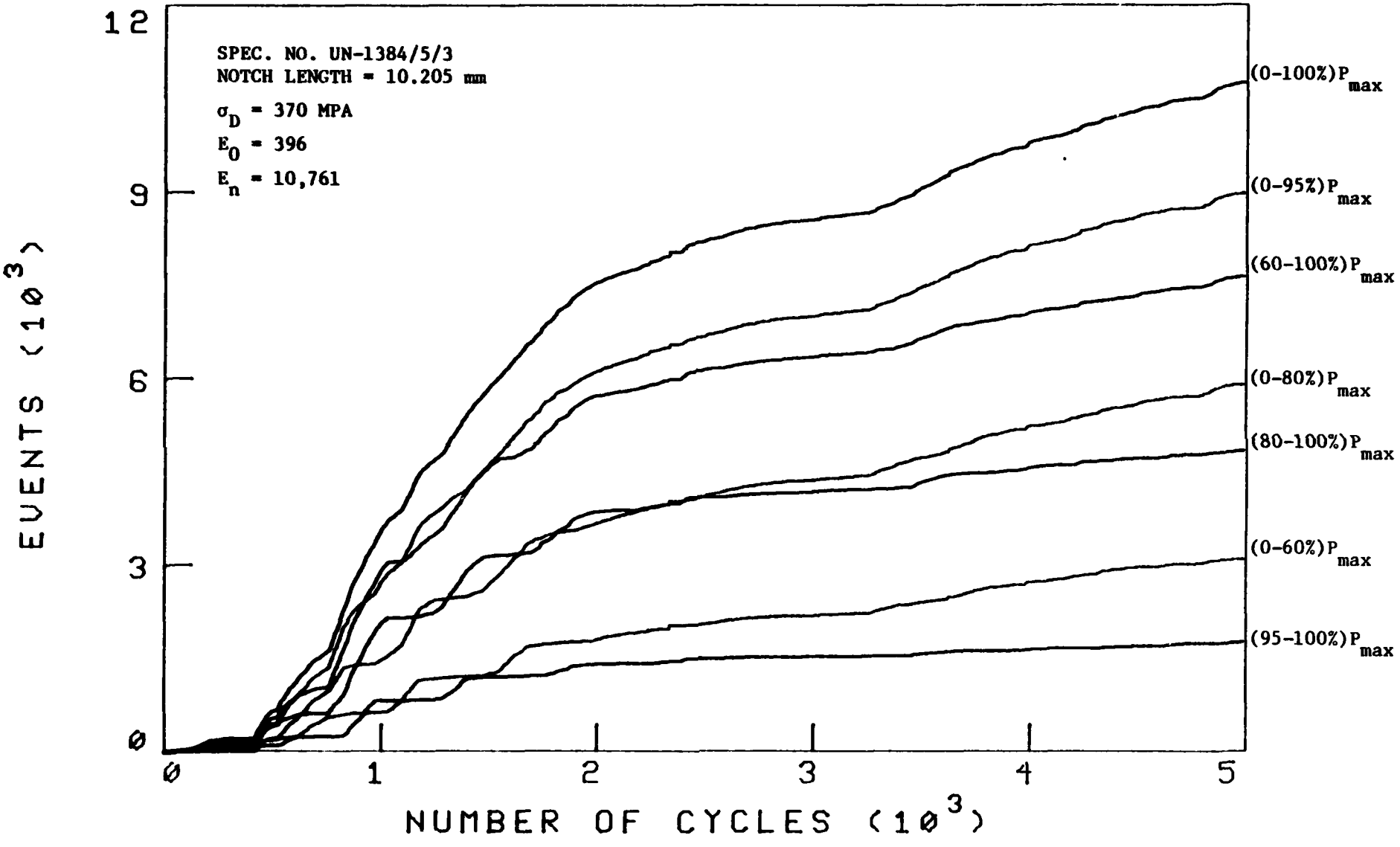

Figure 20. Accumulative number of events as a function of number of cycles accumulated at different load ranges for notched unidirectional 5.6 mil B/Al 6061F.

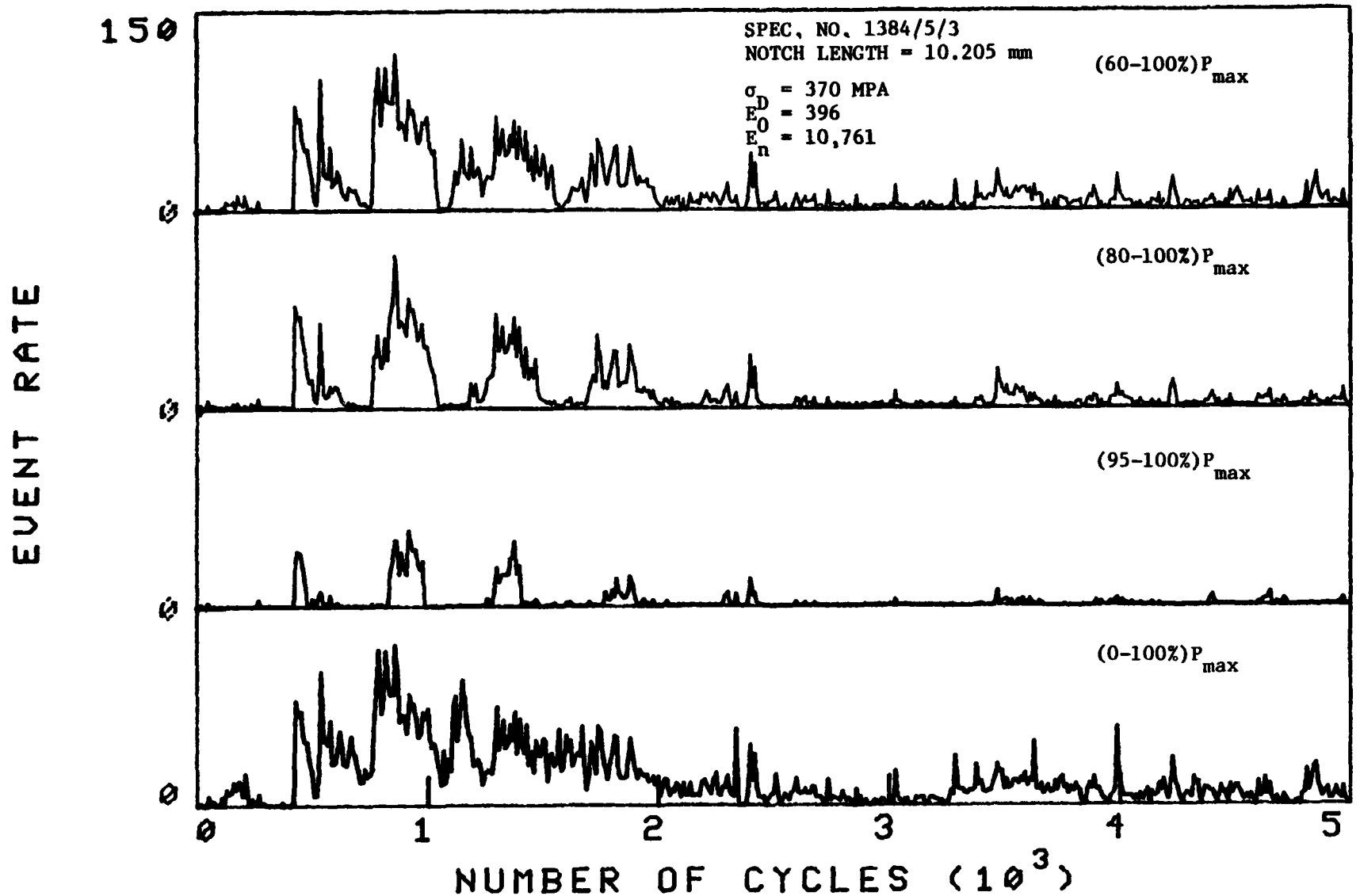

Figure 21. Number of events per ten cycles as a function of number of cycles at different load ranges for notched unidirectional 5.6 mil B/Al-6061F.

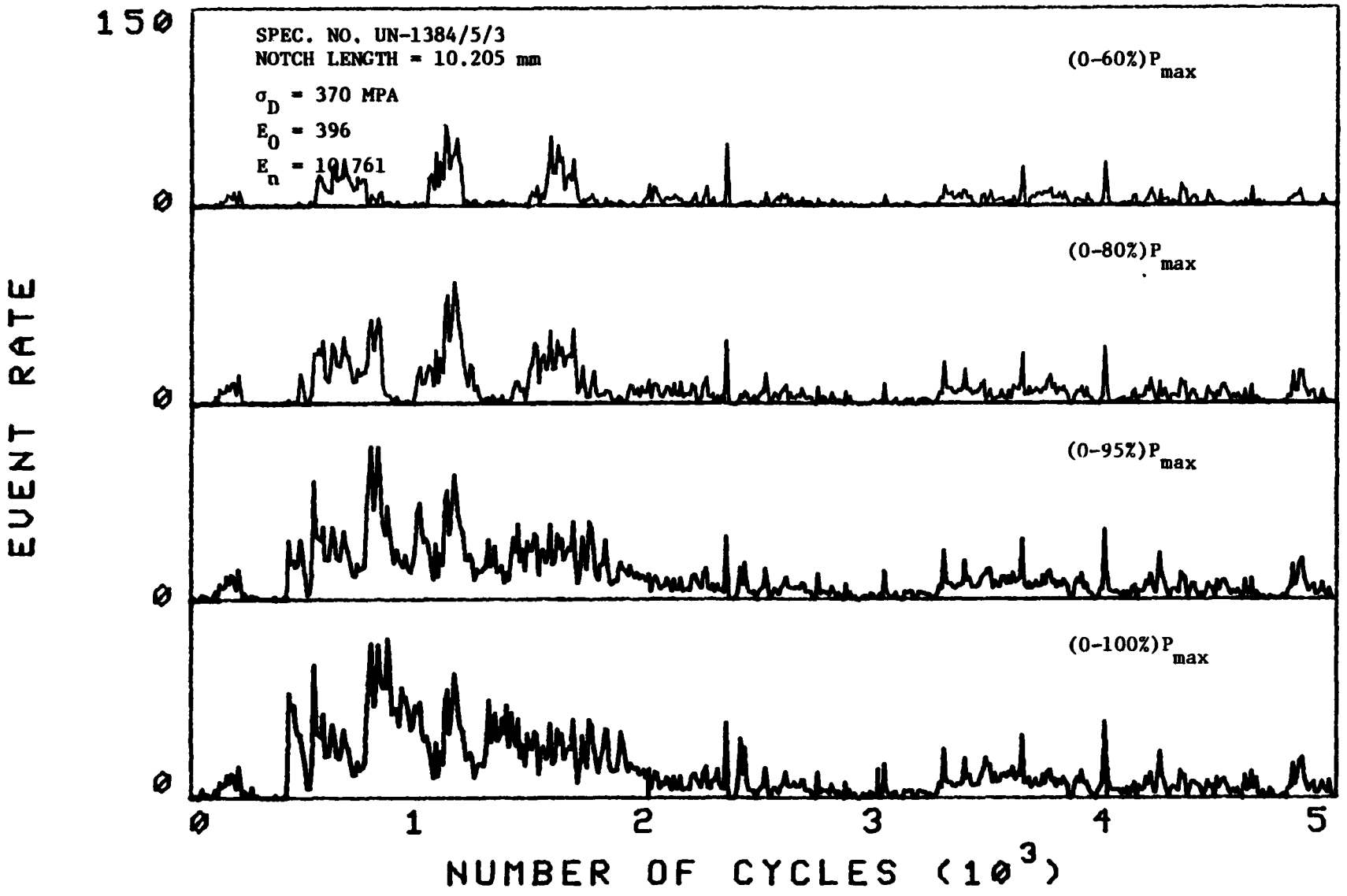

Figure 22. Number of events per ten cycles as a function of number of cycles at different load ranges for notched unidirectional 5.6 mil B/Al-6061F.

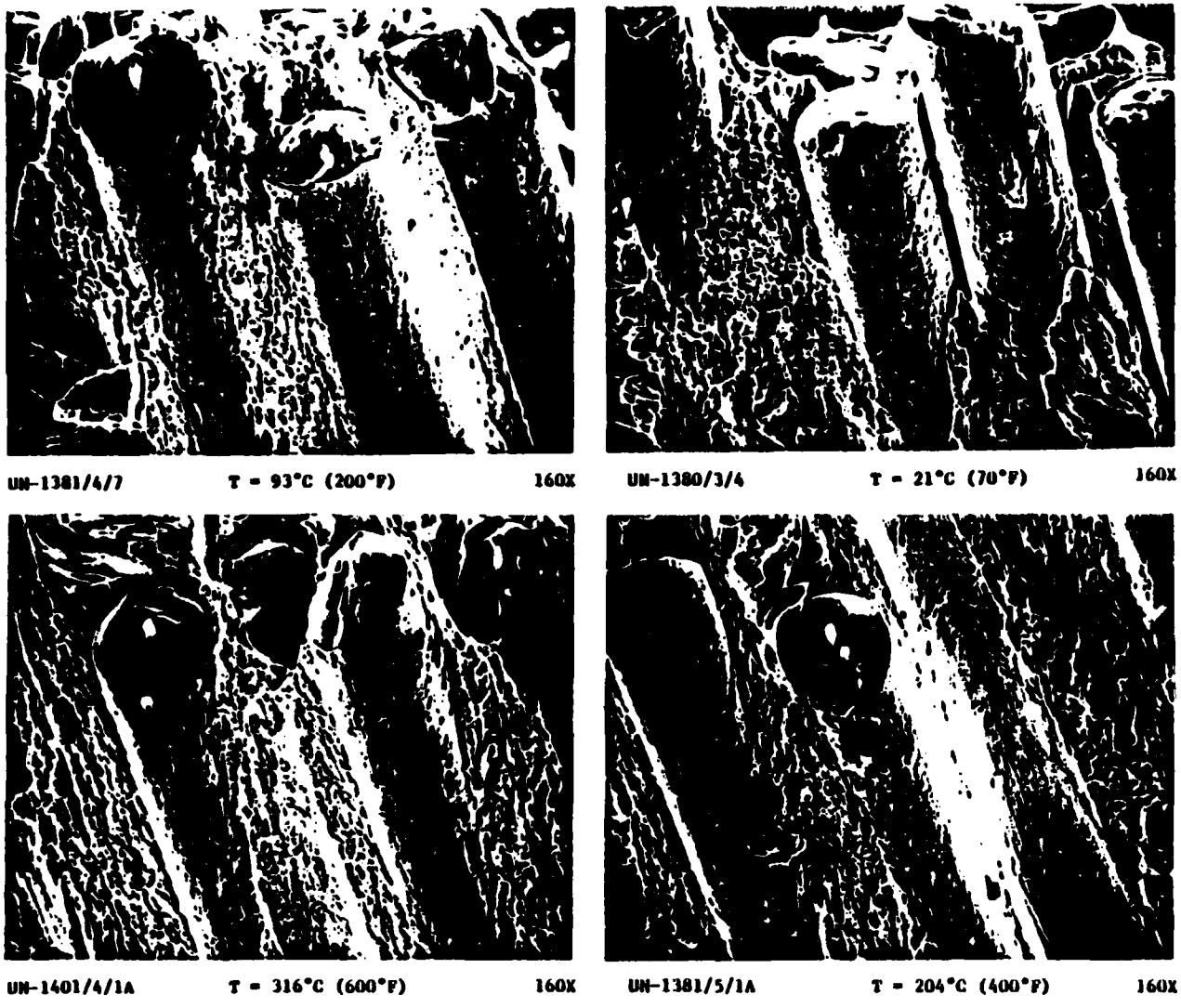

Figure 23. Scanning electron microscope micrographs of fracture surfaces of the splitting area of unidirectional 5.6 mil B/Al-6061F specimens tested at different temperatures.

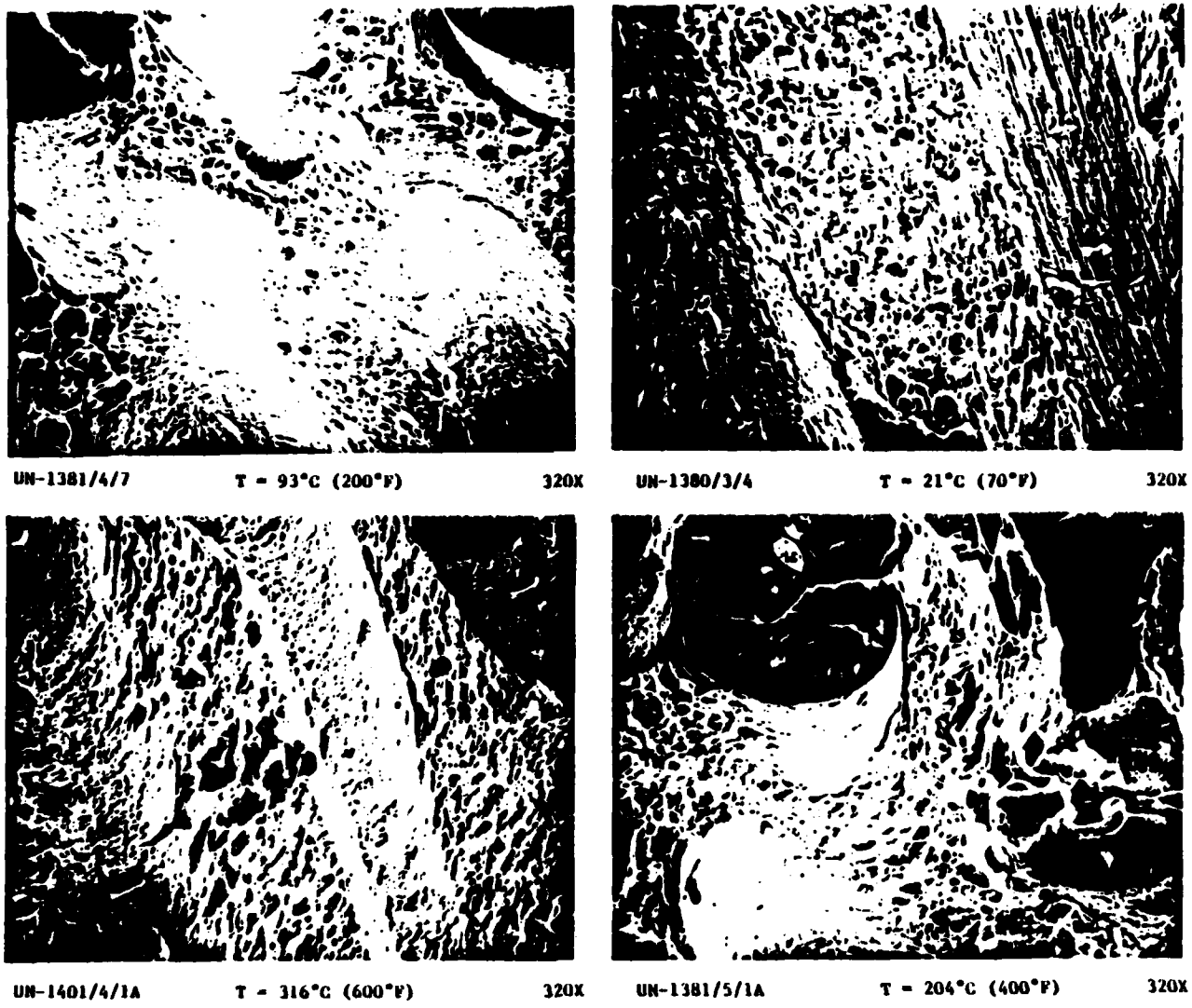

Figure 24. Details of scanning electron microscope micrographs of fracture surfaces shown in Figure 23.

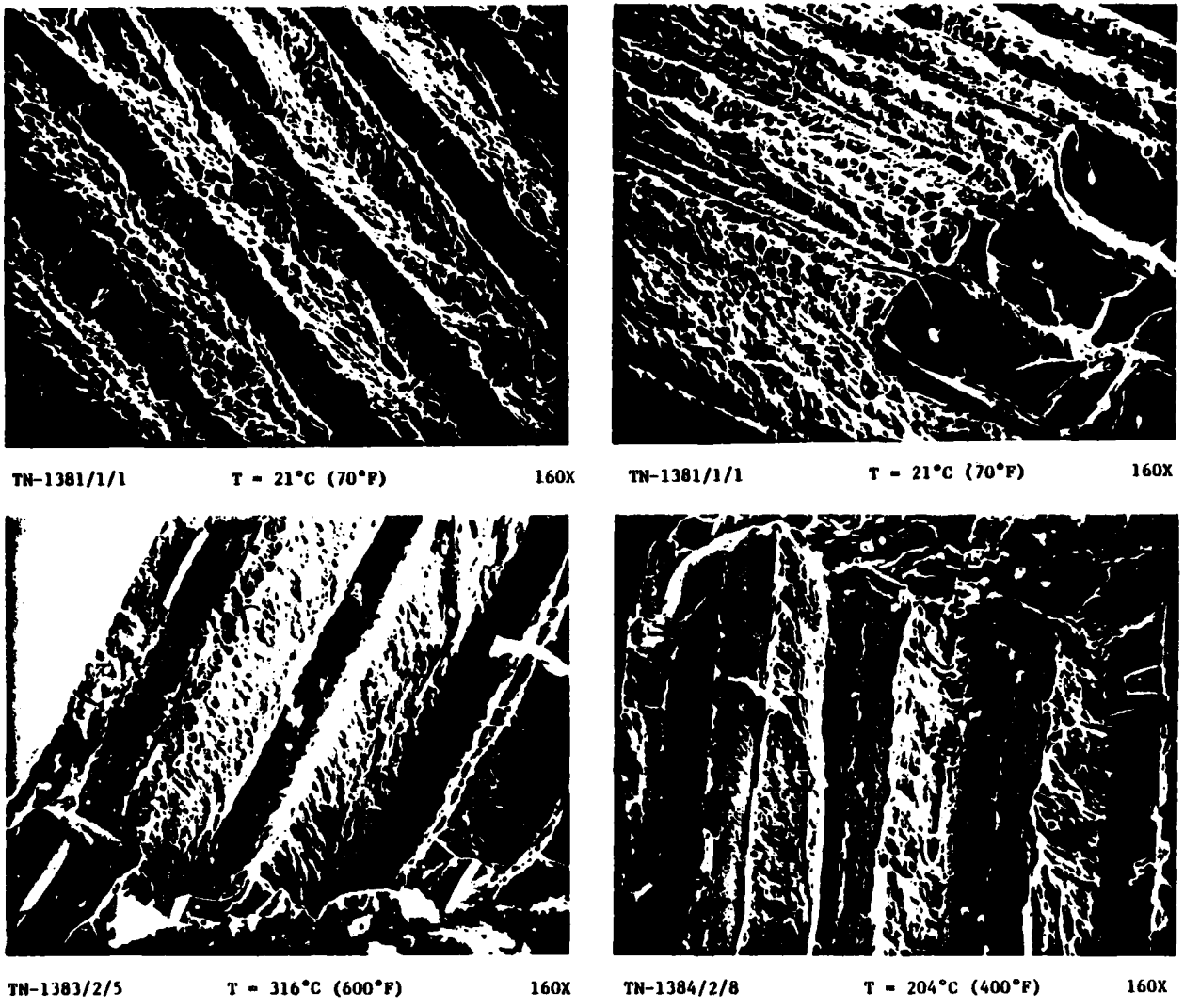

Figure 25. Scanning electron microscope micrographs of fracture surfaces of transverse $[90^{\circ}]_8$ 5.6 mil B/Al-6061F specimens tested at different temperatures.

END

FILMED

5-83

DTIC